Chromatography **2014**, *35*, 1-22

Focusing Review

Highly Sensitive Methods Using Liquid Chromatography and Capillary Electrophoresis for Quantitative Analysis of Glycoprotein Glycans

Shigeo SUZUKI*

Faculty of Pharmaceutical Sciences, Kinki University, 3-4-1 Kowakae, Higashi-osaka, Osaka 577-8502, Japan

Abstract

This review summarizes our recent works concerned on the analysis of glycoprotein glycans. Glycoprotein glycans are highly complicated and have variations that number into the thousands. Therefore the method for their analyses should be carefully chosen according to the complexity and quantity of glycans in samples. To shorten the time for the preparation of labeled glycans from glycoprotein, we proposed two methods: PNGase F/NBD-F method enables the preparation of fluorescently labeled glycans from glycoproteins about 2 hr. A combination of a neutrally coated capillary and borate buffer eliminates the purification steps for the removal of excess reagents from the glycan samples for capillary electrophoresis. Partial filling affinity capillary electrophoresis using glycan-recognizing proteins such as lectins, glycosidases and immunoglobulins, was used for the structural analysis of glycans. The method was applied to the specific detection of NeuGc and α-Gal containing glycans known as the heterogenic antigens. Sensitivity of the detection of glycoprotein glycans separated by microchip-based electrophoresis was enhanced by *in situ* fabricated sufonate-type polyacrylamide gel. This method enhances the sensitivity by a factor of 10^5. *In situ* fabrication of lectin impregnated gels enables specific entrapment and analysis of glycans. Conversion reaction from fluorescently labeled glycans (1-amino-1-alditols) to free oligosaccharides will be helpful for the functional analysis of glycans.

Keywords: Glycoprotein glycans; Fluorimetric detection LC; Laser-induced fluorescent capillary electrophoresis; Microchip electrophoresis; Reductive amination reaction

1. Introduction

The carbohydrate chains found in various biomolecules are the products of diverse posttranslational modifications resulting from the concerted actions of a series of glycosidases and glycosyltransferases existing in the endoplasmic reticulum and Golgi apparatus. It is estimated that over 70% of all human proteins are glycosylated [1]. Glycosylation is often observed on cell surfaces and in extracellular matrices, creating a cellular environment conducive to desired biological interactions [2]. The variation in glycan structures induces changes in the parent molecules, including in peptide chain folding, stability, immune response, and other pathological responses [3]. Moreover, glycan biosynthesis is significantly affected by disease states, and the expression of glycans with specific structures indicates particular pathological states. Therefore, the expressions of specific glycans are now recognized as key steps for certain immune responses caused by disease and several cancers [4,5].

The determination of the structure of glycans is very important in clinical diagnosis. However, the prediction of the glycan structures is impossible based on genomic techniques, because glycans are the products of multiple sequential and competitive enzymatic actions. Therefore, understanding the function of glycans and their changes in relation to disease is an important field of biological analysis, which is often referred to glycomics and glycoproteomics.

This paper describes our recent works using HPLC and capillary electrophoresis (CE) for the quantitative and sensitive analysis of oligosaccharides and component monosaccharides in glycoproteins.

2. High throughput analysis of *N*-linked oligosaccharides of glycoproteins

2.1. PNGase F/NBD-F method for rapid preparation of

*Corresponding author: Shigeo SUZUKI
Tel: +81-6-4307-4004; Fax: +81-6-6721-2353
E-mail: suzuki@phar.kindai.ac.jp

fluorescently labeled oligosaccharides from glycoproteins [6]

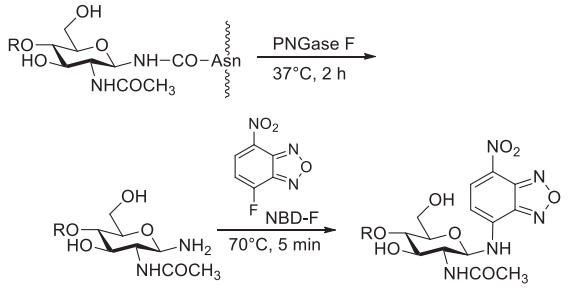

Scheme 1. Enzymatic release of glycosylamine-type oligosaccharides by the action of PNGase F and their derivatization with 4-fluoro-7-nitrobenzofurazan (NBD-F).

PNGase F has been used for releasing asparagine-linked oligosaccharides from glycoproteins. If a glycoprotein is incubated with PNGase F, the amide linkage between an oligosaccharide and asparagine in a peptide sequence is hydrolyzed to form β-glycosylamine-type oligosaccharides and aspartic acid [7]. β-Glycosylamine oligosaccharides are gradually converted to free oligosaccharides in the solution. The stability of the glycosylamine is dependent on the pH of the reaction solution. Glycosylamine oligosaccharides are stable at weak alkaline media (pH ≈ 8.0), and the rate of hydrolysis from the glycosylamine to free oligosaccharide is very slow [8]. The overall reaction scheme is depicted in Scheme 1. Glycosylamine oligosaccharides in the digestion mixture can be derivatized with amine-labeling reagents. This strategy has two advantages. Firstly, the derivatives of glycosylamines have a single configuration (*i.e.* β-form) at the reducing end, and have no isomers that complicate the chromatograms. Second, one-by-one relationship between labeling tag to glycans enables to obtain quantitative profiles of glycans directly from chromatograms.

NBD-F was proposed for labeling glycosylamines because the reaction of amines with this reagent proceeds under the slightly basic conditions. Moreover NBD-labeled glycosylamine fluoresces at 480 nm of Ar laser, which is frequently used for as a light source for fluorimetric detection of femtomole amounts of glycans.

2.1.1. Optimization studies for the labeling of glycosylamine oligosaccharides released from glycoprotein samples

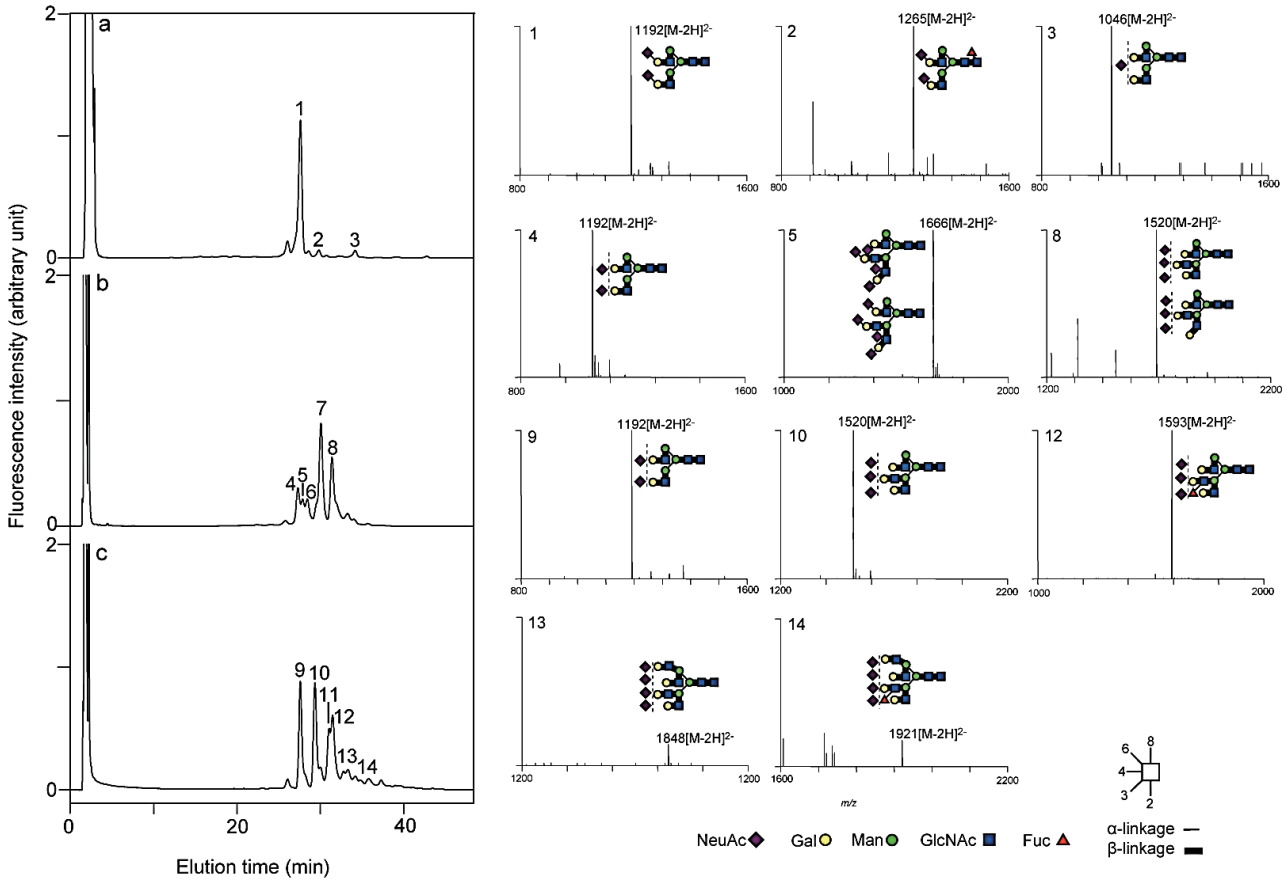

Fig. 1. Application of the PNGase F/NBD method for the HPLC analysis using fluorometric detection of oligosaccharides from human serum transferrin (a), fetal calf serum fetuin (b), and human α_1-acid glycoprotein (c) with ESI-MS spectra of each peak.

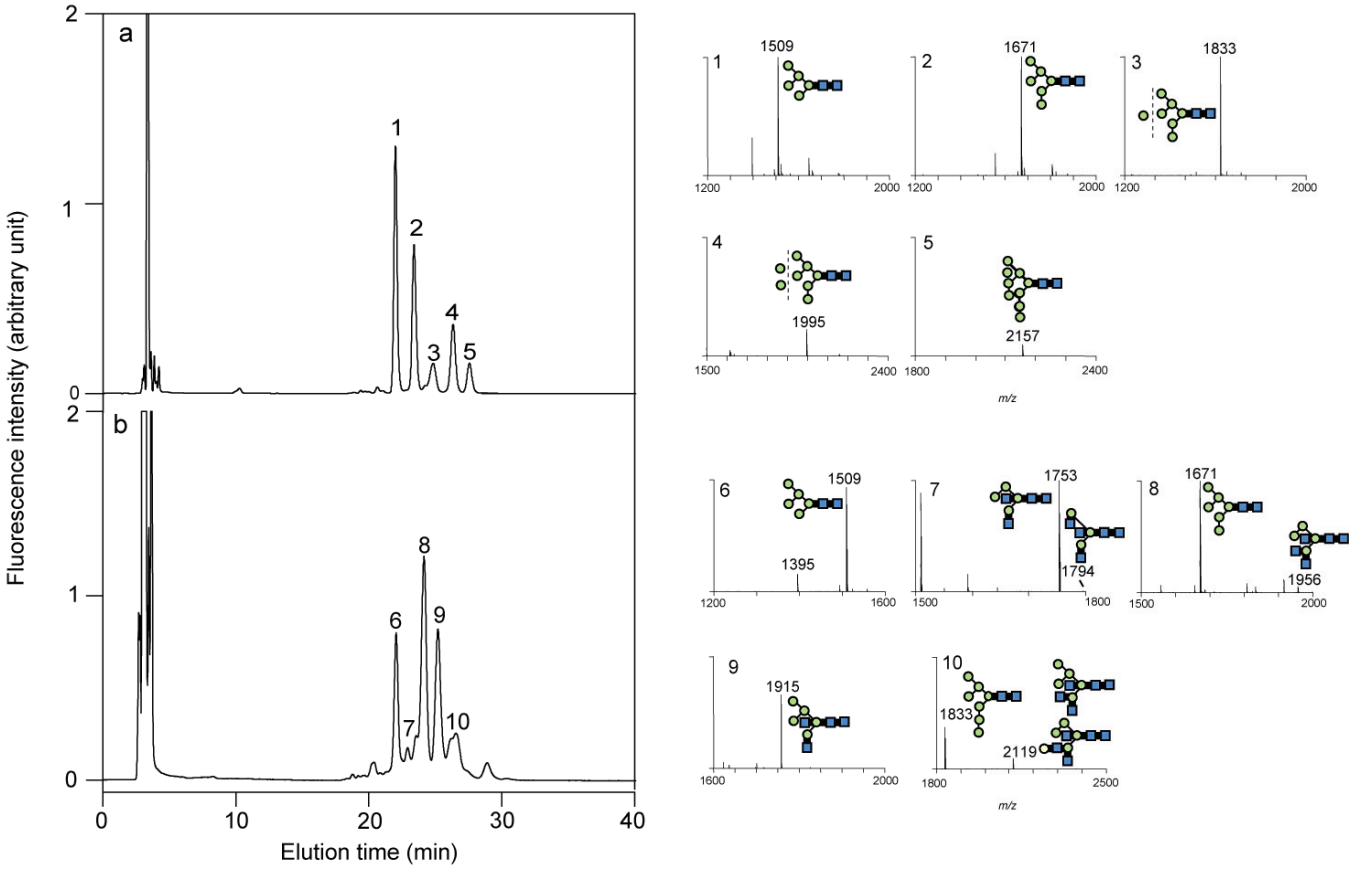

Fig. 2. Application of the PNGase F/NBD method for the HPLC analysis of oligosaccharides from bovine ribonuclease B (a) and ovalbumin (b).

PNGase F/NBD-F method was optimized using human serum transferrin as a model glycoprotein. The buffer pH was optimal at 8.0. The concentration of buffer was not so critical but seemed to be optimal at 20–100 mM of phosphate (pH 8.0), the reaction rate of NBD labeling was enhanced with reagent concentration, and almost reached a plateau at 300 mM NBD-F solution. The reaction was completed within 5 min at 70°C using 300 mM NBD-F. A 2 h reaction of PNGase F in 20 mM phosphate buffer (pH 8.0) and labeling with 300 mM NBD-F at 70°C for 5 min was chosen as the optimal conditions for derivatization. The repeatability of this method based on the peak area of samples independently prepared from 50 μg of transferrin was 4.1% (n = 5) as RSD. Under the optimized conditions, more than 90% of oligosaccharides were converted to NBD-labeled glycans. The detection sensitivity of NBD-labeled oligosaccharides was compared with those of Fmoc- and ethyl *p*-aminobenzoate (ABEE) derivatives. The peak area of NBD derivatives was 4.4 times more intense than that for Fmoc derivatives, and 5.7 times more intense than that for ABEE derivatives.

2.1.2. HPLC analyses of oligosaccharides derived from glycoproteins

PNGase F/NBD-F labeling method was applied to the HPLC analysis of oligosaccharides derived from various glycoproteins. Fig. 1 shows the separation of *N*-linked oligosaccharides derived from human transferrin, bovine fetuin, and human α_1-acid glycoprotein. To confirm the structures of some oligosaccharides, the derivatives were analyzed by LC with fluorimetric detection and ESI-MS. The oligosaccharides were separated according to the molecular sizes and content of sialic acids. The broadening of some peaks appeared in fetuin and α_1-acid glycoprotein may be due to the presence of linkage isomers.

Neutral glycans were separated on a diol column (Fig. 2). High mannose-type oligosaccharides ($Man_{5-9}GlcNAc_2$) from ribonuclease B [9], and series of high-mannose and hybrid oligosaccharides derived from ovalbumin were mainly separated according to their molecular sizes. The oligosacchardies were detected as adduct ion of TFA, $[M+CF_3CO_2]^-$ in ESI-MS. The sensitivities of NBD-labeled oligosaccharides were compared with those of Fmoc- and ABEE-labeled oligosaccharides in negative ESI-MS analyses: they were 12 times and 10 times higher than those for Fmoc and ABEE derivatives, respectively.

2.1.3. Application to CE with laser-induced fluorimetric (LIF) detection

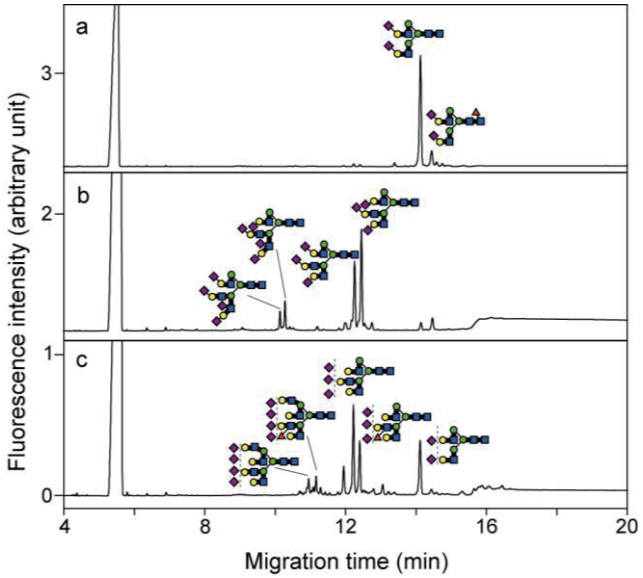

Fig. 3. Capillary electrophoresis with laser-induced fluorometric detection of oligosaccharides derived from transferrin (a), fetuin (b), and α_1-acid glycoprotein (c).

LIF-CE with an argon ion laser was applied to the analysis of NBD-labeled glycosylamine-type oligosaccharides. NBD-labeled oligosaccharides were separated as anionic borate complexes on neutrally coated capillary using 100 mM borate (pH 8.3) as the electrophoresis buffer. The neutrally coated capillary suppresses the generation of electroendoosmotic flow. Therefore, NBD-oligosaccharides move to the anode based on the number of acidic groups (*i.e.,* number of NeuAc residues) and the association with borate ions.

Fig. 3 shows the separation of NBD-labeled oligosaccharides derived from human transferrin, bovine fetuin, and human α_1-acid glycoprotein. Derivatives were separated based on the number of sialic acid residues. Tetrasialo-, trisialo- and disialooligosaccharides appeared at 10–11 min, 12 min and 14 min, respectively. Further resolution seemed to be based on the difference in oligosaccharide structures. The limit of detection of NBD-labeled oligosaccharides estimated from a main peak of transferrin-derived oligosaccharides was 4 fmol (S/N ratio = 20).

2.2. A novel condition for capillary electrophoretic analysis of reductively aminated saccharides without removal of excess reagents

We developed the selective and sensitive separation conditions for profiling monosaccharides and oligosaccharides without the removal of excess reagents. AMC-labeled saccharides have no charge in alkaline buffer. However in the presence of boric acid, the adjacent hydroxyl groups on saccharides form acidic complexes with borate, which provide a strong negative charge to AMC-labeled saccharides and induces their movement toward the anode. This method allows selective quantification of all of component monosaccharides found in glycoprotein hydrolysates and sensitive detection of glycoprotein-derived oligosaccharides at subattomole level.

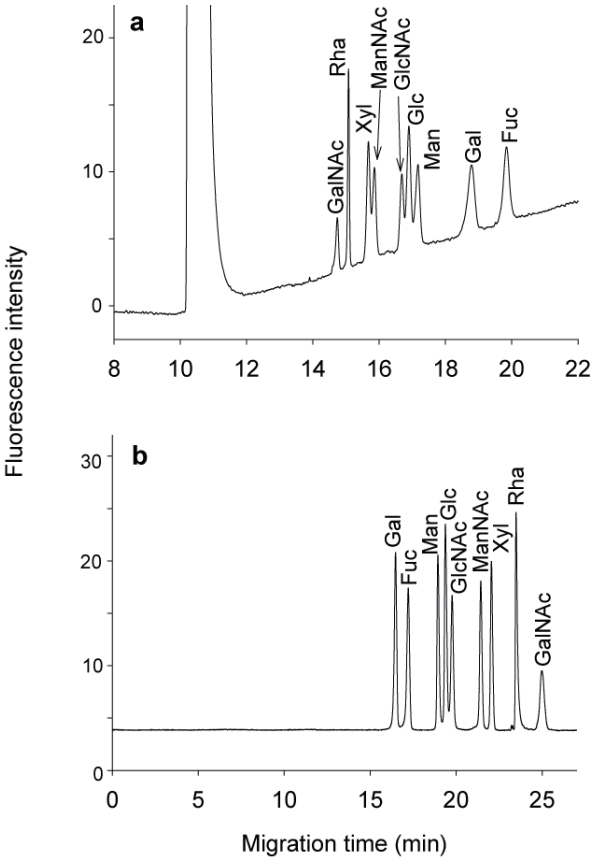

Fig. 4. Fluorescent CE analysis of selected monosaccharides in borate complexation mode using a bare fused silica capillary (a) and a PDMS- coated capillary (b). Analytical conditions: running buffer, ACN and 200 mM sodium borate (pH 9.5) containing 0.05% hydroxypropylcellulose (1:9, v/v); capillary size, 50 μm id × 50 cm (40 cm for detector); capillary temp., 25°C; applied voltage +15 kV (a) and −15 kV (b); detection, fluorescence with 365 nm LED. GalNAc, N-acetylgalactosamine; Rha, rhamnose; Xyl, xylose; ManNAc, N-acetylmannosamine; GlcNAc, N-acetylglucosamine; Glc, glucose; Man, mannose; Gal, galactose; Fuc, fucose.

2.2.1. Optimization of separation conditions for monosaccharide analysis

A PDMS-coated capillary was used instead of a bare fused silica capillary to suppress EOF, and basic borate buffer was used as background electrolytes. In these conditions, saccharide derivatives generate negative charges

as borate complexes, which move toward the anode in an electric field, besides excess reagent and their decomposition products residing in the reaction mixture cannot be charged in alkaline borate buffer. Therefore, the excess reagents in the reaction mixture can be removed from electropherograms without requiring purification before analysis.

The resolution of AMC monosaccharide derivatives depends strongly on the pH of the borate buffer and also the species and concentration of organic solvent. The separation window (*i.e.,* time window for the separation of monosaccharides) is broadened with increasing electrophoresis buffer pH, and the sharpness of AMC monosaccharide peaks increased with the concentration of the borate buffer, and reaching a maximum of over 200 mM. Addition of a water-miscible solvent such as methanol, ethanol, or acetonitrile (ACN) is essential to prepare a clear solution from the AMC reaction mixture because of the low solubility of AMC in water. Among these three solvents, we found that the addition of ACN is preferable in the enhancement of peak resolutions. Baseline resolution was obtained using a 1:9 v/v mixture of ACN and borate buffer containing 0.05% hydroxypropylcellulose. However, the anions residing in the reaction mixture partly diminished the sharpness of specific peaks. To enhance the sharpness of saccharide peaks, acetic acid was added to AMC-labeled sample at a concentration of 0.5 M. Good resolution between the nine monosaccharide derivatives was obtained under the optimized conditions, as shown in Fig. 4b. Linear quantitation ranges were obtained over the concentration range between at least 0.4 and 400 μM (calculated to be 140 amol to 140 fmol), and 80 nM (*ca.* 28 amol) as the LOD (S/N = 5).

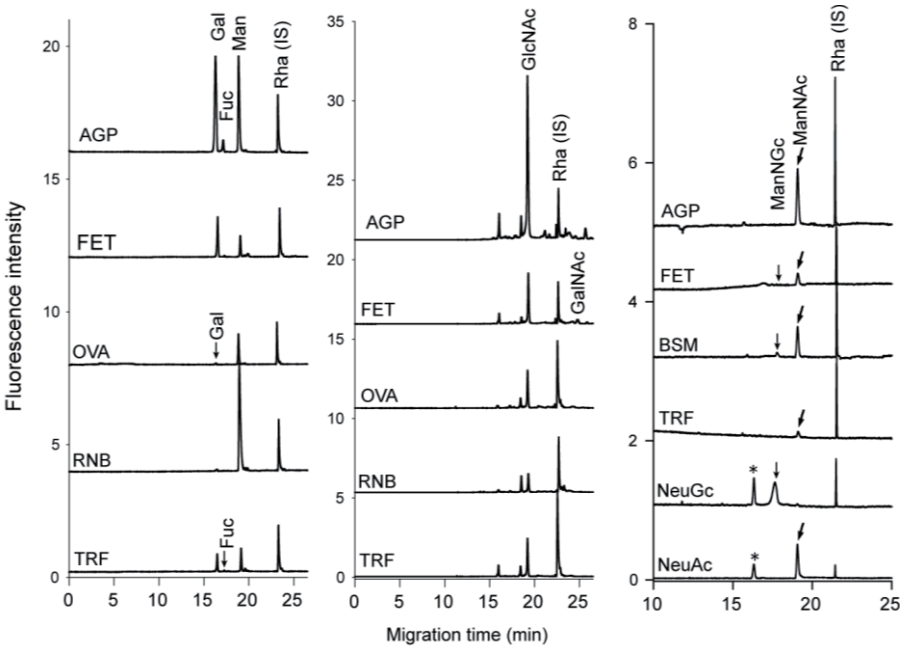

Fig. 5. Analysis of component monosaccharides in hydrolysates of various glycoproteins. Analytical conditions were the same as those used for Fig. 4b. ManNGc and ManNAc were derived from NeuGc and NeuAc, respectively. AGP, acid glycoprotein; FET, fetuin; OVA, ovalbumin; RNB, ribonuclease B; TRF, transferrin; BSM, bovine submaxillary mucin.

Table 1. Estimated content (%) of monosaccharides in various glycoprotein specimens

Glycoprotein	Man	Gal	GlcNAc	GalNAc	NeuAc	NeuGc	Fuc
α1-Acid glycoprotein	5.80	8.99	13.88	N.D.	10.02	N.D.	0.47
	5.50	7.60	13.20	N.D.	10.90	N.D.	0.70
Fetuin	1.60	3.15	4.26	1.30	6.28	0.68	0.04
	2.45	3.49	2.62	0.54	4.62	–	0.03
Transferrin	1.15	0.76	1.27	N.D.	0.91	N.D.	0.07
	1.08	1.00	1.79	0.05	1.40	N.D.	
Submaxillary mucin	–	–	–	–	5.80	4.59	–
	–	–	–	–	1.69	1.25	
Ovalbumin	2.47	0.11	1.63	N.D.	N.D.	N.D.	N.D.
	2.80	0.12	0.28	N.D.	N.D.	N.D.	N.D.
RibonucleaseB	4.63	N.D.	1.09	N.D.	N.D.	N.D.	N.D.
	2.20	N.D.	0.91	N.D.	N.D.	N.D.	N.D.

Values appearing on the lower line for each glycoprotein indicate reference values.
N.D.: not detected; –: not determined.

2.2.2. Analysis of component monosaccharides in glycoproteins

The optimized conditions were applied to the analysis of component monosaccharides in a number of glycoproteins.

Saccharide chains in glycoproteins comprise Man, Gal, Fuc, GlcNAc, GalNAc, NeuAc, and NeuGc. Monosaccharides are released by acid hydrolysis with 2 M TFA for neutral aldoses and 4 M HCl for hexosamines for quantitative recovery [15]. Sialic acids are enzymatically released and the generated neuraminic acids were further converted to *N*-acetyl- or *N*-glycolylmannosamine derivatives by the action of aldolase [16]. Fig. 5 shows the results of monosaccharide analysis of several glycoprotein samples. Based on the peak area of each sample relative to rhamnose as a internal standard, the monosaccharide contents were estimated and are summarized in Table 1. The results were compared to those of previously reported data [16,17]. The removal of the purification step for derivatives could enhance the reliability of quantitation for saccharides in glycoconjugate samples.

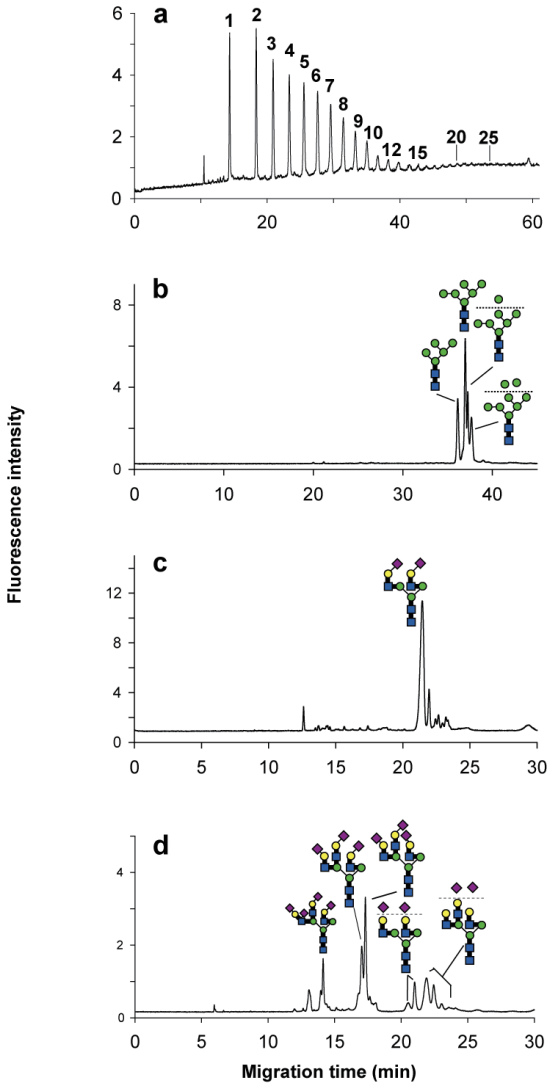

Fig. 6. Separation of a mixture of isomaltooligosaccharides (a), and glycans from ribonuclease B (b), transferrin (c), and fetuin (d). Running buffer, 1:9, v/v, mixture of ACN and borate buffer containing 0.5% hydroxypropylcellulose; 250 mM potassium borate (pH 9.0) for (a) and (b), and 100 mM Tris borate (pH 8.5) for (c) and (d), respectively.

Our data may therefore be more reliable than that from previously reported methods and, moreover, the sensitivity is far superior to previous methods.

2.2.3 Analysis of oligosaccharides in glycoproteins

Analytical conditions for oligosaccharides were tuned by using AMC-labeled isomaltooligosaccharides, and found 250 mM potassium borate buffer (pH 9.0) most optimal. As shown in Fig. 6a, they were completely resolved and oligosaccharides corresponding to DPs of more than 20 were detected within 60 min. The separation conditions were applied to the analysis of AMC-labeled *N*-linked oligosaccharides from transferrin, fetuin, and ribonuclease B. However, the separation of acidic oligosaccharides derived from transferrin and fetuin indicates finer resolution using a somewhat lower pH of borate buffer. Therefore, we applied 100 mM Tris borate (pH 8.5) for acidic oligosaccharide separation. Results are shown in Fig. 6c,d. Neutral oligosaccharides migrated in order of their size, and acidic oligosaccharides were mainly separated according to the number of sialic acids and were further resolved by the linkage type and position as well as differences in the lactosamine linkage.

2.2.4 Application to the separation of saccharides using other labels

This method were also applied to the separation of monosaccharides and isomaltooligosaccharides labeled with other fluorescent tags. Saccharides labeled with 2-aminoacridone (AMAC) and ethyl *p*-aminobenzoate (ABEE) showed an essentially identical pattern to AMC saccharides and were also free from interference by excess reagents (Fig. 7).

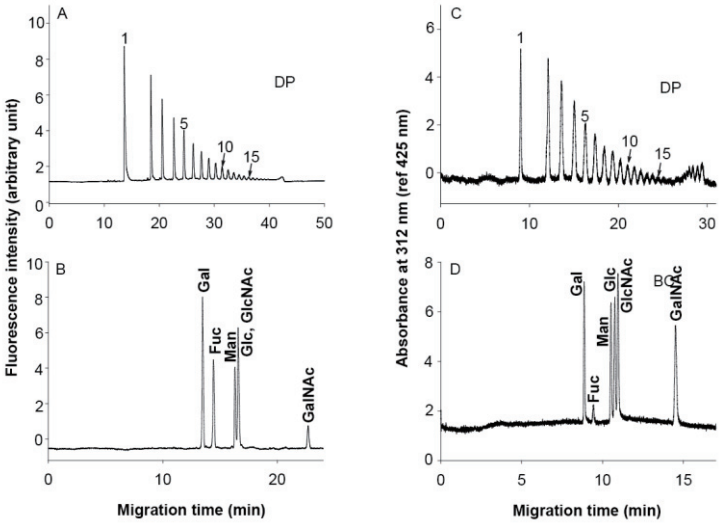

Fig. 7. Application to the separation of isomaltooligosaccharides and monosaccharide mixtures labeled with AMAC (A, B) and ABEE (C, D).

3. Partial filling affinity capillary electrophoresis for glycan profiling

Affinity capillary electrophoresis (ACE) is a version of CE, and has been used to examine various biological interactions [18–22]. ACE using carbohydrate recognition proteins, such as lectins has certain advantages in the glycobiology era. Previously lectin ACE have been reported to demonstrate the usefulness in the determination of the specific structure of oligosaccharides, but the concentration, components and pH of the electrophoresis buffers have limited to sustain activity of the lectin used, and the usage of protein-containing buffers can complicate analyses due to adsorption of proteins to the capillary, vials and electrodes. A partial-filling ACE [23] can be used to overcome these situations.

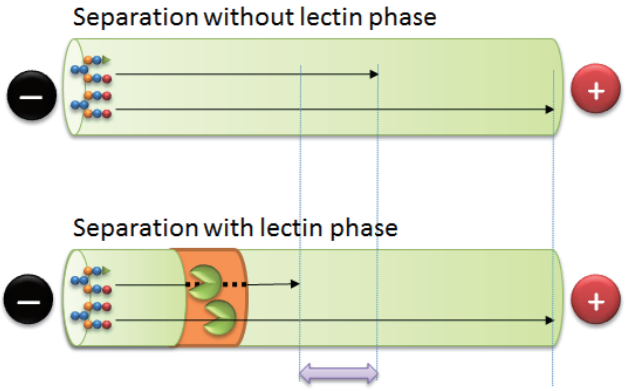

Fig. 8. Image of partial-filling affinity capillary electrophoresis of APTS-labeled oligosaccharides with lectins using a neutrally coated capillary. A specific delay shown as a bidirectional arrow indicates interaction with lectin partially filled in a capillary.

Fig. 8 portrays the experimental design of partial-filling ACE. A lectin solution and then oligosaccharides labeled with 8-aminopyrene-1,3,6-trisulfonic acid (APTS) were hydrodynamically introduced to a neutrally coated capillary filled with electrophoresis buffer. Lectins with a high molecular mass had minimal electrophoretic velocity in a neutral background solution. In contrast, APTS derivatives, having three sulfonate groups, induced a high velocity in electric field. By applying a negative voltage to the capillary, APTS-labeled oligosaccharides quickly moved to the anode based on their size-to-charge ratio and passed through a zone of lectin solution. APTS oligosaccharides recognized by the lectin were slowed down in the lectin plug depending on affinity strength and complex mobility. The migration times were increased and often accompanied by peak broadening. In contrast, APTS oligosaccharides having no affinity for the lectin migrated with constant velocity over the capillary, and their elution profile did not change in the presence of lectin. Therefore, alteration of electrophoretic profiles in the presence of lectins directly indicated the affinity of specific oligosaccharides to the lectin.

3.1.2. Partial-filling lectin ACE of a mixture of high mannose and complex-type oligosaccharides derived from porcine thyroglobulin

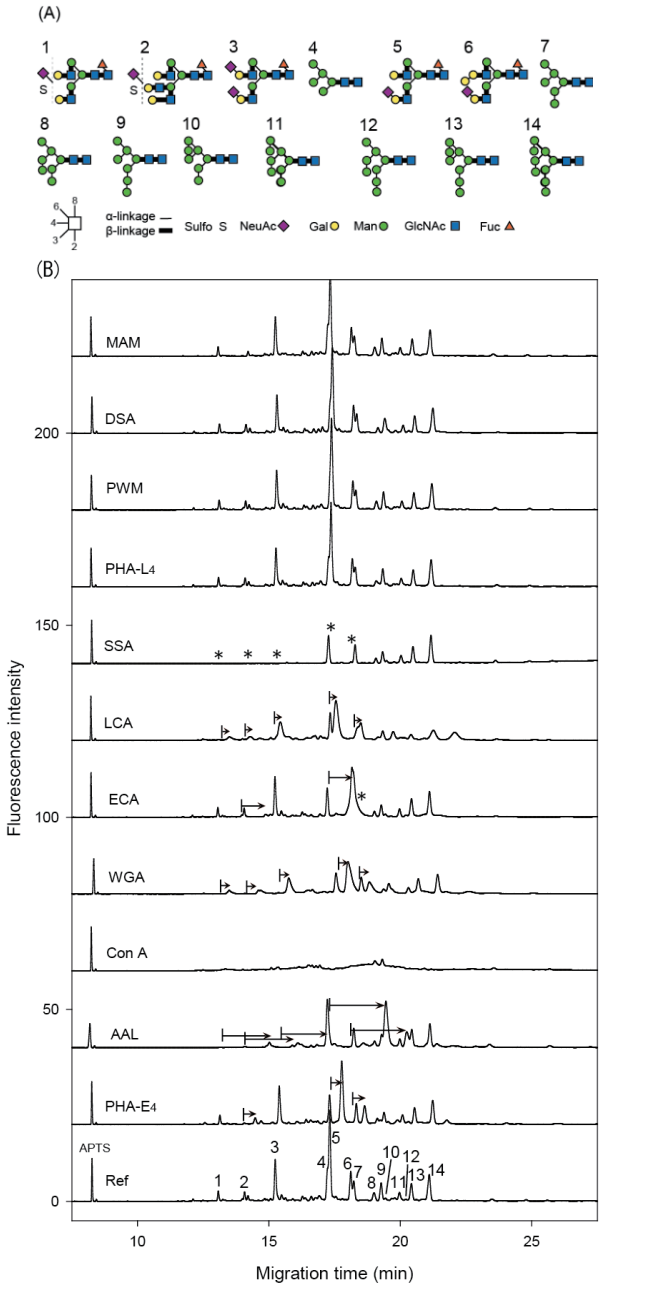

Fig. 9. Oligosaccharide structures previously reported and tentative assignment of peaks (A) and partial-filling affinity capillary electrophoresis of APTS-labeled oligosaccharides derived from porcine thyroglobulin with various lectins (B).

Porcine thyroglobulin was chosen as an oligosaccharide pool (Fig. 9(A)) [24–27], and applied to study interaction of

various lectins. Each lectin was dissolved in the running buffer at 1 mg/mL (10–30 μM), and introduced at 3.45 kPa for 30 s. Migrations of the oligosaccharides in the presence of lectins are shown in Fig. 9(B). MAM recognizes complex-type glycans containing α2,3-linked NeuAc [28]. DSA is specific to polylactosamine and tetraantennary oligosaccharides [29]. PWM is specific to *N*-acetyllactosamine [30], and PHA-L_4 recognizes some tri- and tetraantennary oligosaccharides [31,32]. Electropherograms obtained in the presence of these lectins were approximately identical to the reference electropherogram shown at the bottom of Fig. 2(B). ACE using other lectins showed specific migration profiles. SSA recognizes α2,6-linked NeuAc [33], and causes complete dissipation of peaks 1 to 3, 5, and 6. LCA has affinity for biantennary oligosaccharides with α1,6-linked Fuc in its core [34]. Severe broadening and slight retardation (*ca*. 10 s) of peaks 1 to 3, 5, and 6 indicates the presence of these structures. Peak 2 and peak 5 were apparently retarded *ca.* 40 s by the addition of β-linked Gal specific ECA [35]. Peaks 1 to 3, 5, and 6 were recognized by β-GlcNAc and NeuAc specific WGA [36]. All complex type glycans were recognized and their migration times were increased *ca.* 2 min by Fuc-specific AAL [37]. The peaks were assignable to complex-type oligosaccharides containing Fuc residues. PHA-E_4 recognizes biantennary oligosaccharides and triantennary oligosaccharides having two lactosamine branches at α1,3-linked Man; their affinity is reduced by the presence of terminal sialic acids [38]. From comparison of the reference electropherogram, the migration times of peaks 2, 5, and 6 were increased by ~30 s, which indicated that these peaks were trapped by this lectin and were assignable to biantennary oligosaccharides with terminal Gal residues. As shown above, lectins recognize specific oligosaccharides in oligosaccharide pools.

3.1.3. Multiple-injection analyses

Partial filling ACE using a series of lectins can be realized by injecting a series of lectin solution sequentially into the capillary before the analysis. We chose porcine thyroglobulin as a model oligosaccharide pool and tried specific detection of high-mannose-type oligosaccharides from a pool including a series of complex-type oligosaccharides. To trap all complex-type glycans, we chose four lectins: α2,3-NeuAc-specific MAM, α2,6-NeuAc-specific SSA, β-Gal-specific ECA, and α-Fuc-specific AAL. These four lectins were injected at 3.45 kPa for 30 s in this order. Thyroglobulin oligosaccharides were then injected and separated. The separation profile is shown in the upper panel of Fig. 10 which shows only selected peaks. Moreover, the upper trace was very similar to the separation of APTS-labeled high-mannose-type oligosaccharides [39]. This technique can be used to specifically detect oligosaccharides in a complex mixture.

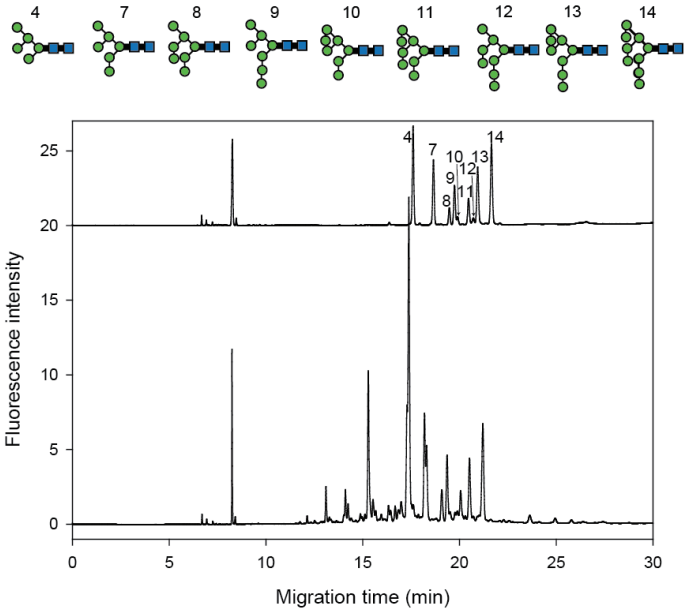

Fig. 10. Partial-filling affinity capillary electrophoresis using a series of lectins to identify high-mannose type oligosaccharides in an oligosaccharide pool derived from porcine thyroglobulin. The lower trace shows the reference data obtained without lectins.

3.1.4. Partial filling affinity capillary electrophoresis using large-volume sample stacking with an electroosmotic flow pump for sensitive profiling of glycoprotein-derived oligosaccharides [40,41]

'Large-volume sample stacking with an electroosmotic flow pump' (LVSEP) is a preconcentration technique used for the analysis of analytes introduced in the whole of a separation capillary [42]. The method seems useful in PFACE for the analysis in minute amount of glycans in complex mixture. The overall LVSEP-partial filling ACE (LVSEP-PFACE) scheme is shown in Fig. 11. A diluted sample solution of APTS-labeled oligosaccharides is introduced into the entire PDMS-coated capillary (Fig. 11a), then the outlet of the capillary is immersed in a lectin solution and a pressure of 3.45 kPa is applied to introduce a lectin solution as a short plug (Fig. 11b). Then, both ends of the capillary are immersed in electrophoresis buffer and the separation voltage is applied (Fig. 11c). Electroendosmosis in the PDMS-coated capillary is negligible because of the minimal tendency to possess electrical charge. The low concentration of electrolytes in the sample solution induces an electrical charge on the capillary and causes apparent endoosmotic flow (EOF) from anode to cathode (*i.e.*, from outlet to inlet of the capillary) with an EOF velocity of 0.65 mm/s. The EOF velocity decreases gradually as the more high ionic strength electrophoresis buffer solution enters from the outlet of the capillary (Fig. 11d). Concomitantly, the

APTS-labeled saccharides will migrate faster toward the anode and are concentrated in the lectin plug. As the electrophoresis buffer approaches the inlet of the capillary and most of the sample matrix is removed from the cathodic end, the EOF becomes negligible, consequently enabling the APTS-labeled oligosaccharides to be separated based on their molecular size, charge as well as the affinity to the lectin (Fig. 11e). The concentration factor of this method reaches about ~900.

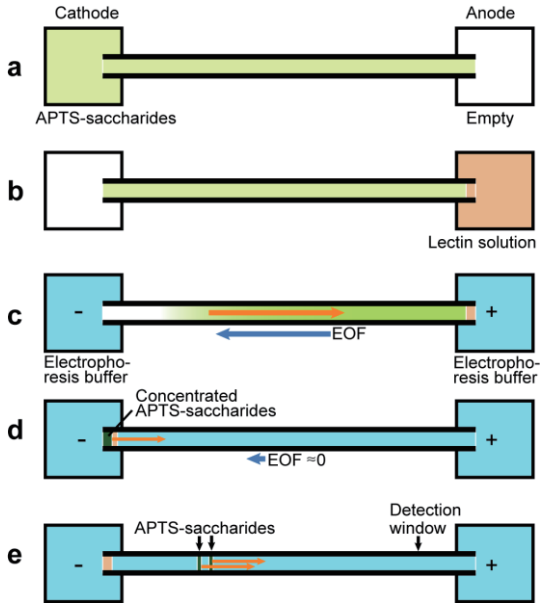

Fig. 11. Image of large-volume sample stacking with partial-filling affinity capillary electrophoresis of APTS-labeled oligosaccharides with lectins, using a neutrally coated capillary. A PDMS-coated capillary was filled with APTS-saccharides solution (a). A lectin solution was injected from the outlet (b). Both ends of the capillary were immersed in electrophoresis buffer and a negative voltage applied (c). APTS-saccharides are enriched at the lectin plug, while the high EOF removes sample matrix from the cathodic end (d). EOF becomes negligible and APTS saccharides are separated by zone electrophoresis (e).

Long time interaction in LVSEP-PFACE indicates drastic change in the separation profile. As previously described, Con A and SSA in ordinary PFACE indicated disappearance of specific peaks as the same as LVSEP-PFACE. However, study using other lectins, AAL, ECA, WGA, LCA and PHA indicated disappearance of the peaks. These lectins indicated an increase in the migration times of specific peaks from 30 s to 2 min in ordinary PFACE (Fig. 9). The difference may be due to the effectiveness of the affinity interaction in LVSEP-PFACE. The increase in the residence time in the lectin phase in LVSEP-PFACE enhances the efficiency of the interaction.

LVSEP injection and ordinary injection in PFACE analysis was compared by evaluating the efficiency by changing the injection volumes of lectin in each by using immunoglobulin oligosaccharides and Fuc-specific AAL as a lectin. Results are shown in Fig. 12. For the LVSEP-PFACE, the peak intensities of oligosaccharides were reduced with increasing injected amount of lectin (left in Fig. 12). In contrast, ordinary PFACE indicates a gradual broadening and retardation with increasing injection amount of AAL (right in Fig. 12). In LVSEP-PFACE, APTS-saccharides are concentrated in the lectin plug for 2.3 min, while the saccharides were continuously supplied from the sample phase and were retained based on the difference in the concentrations of the electrolytes. Therefore, the advantage of combining the LVSEP mode with PFACE is that the sensitivity is enhanced as well as the interaction efficacy of lectins.

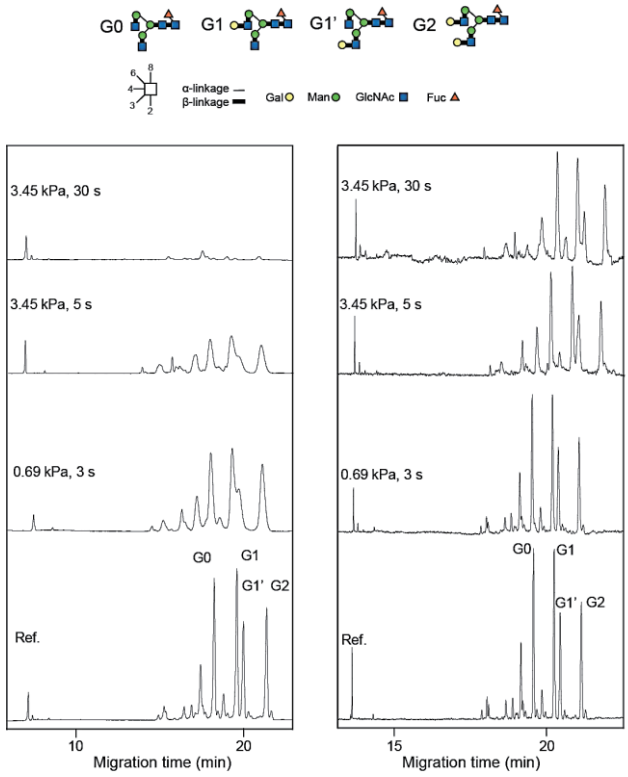

Fig. 12. Comparison of LVSEP-PFACE (left) and ordinary PFACE (right) analysis of APTS-labeled oligosaccharides from immune-globulin with AAL. Lectin injection conditions are shown in each electropherogram.

3.1.5 Application of partial-filling capillary electrophoresis using lectins and glycosidases for the characterization of oligosaccharides in a therapeutic antibody [43,44]

Antibodies are becoming important agents for medical treatment because of their high specificity and low toxicity. Antibody molecules contain glycosylation sites, which bear various oligosaccharides depending on the cell lines used for antibody production [45, 46]. The structures of oligosaccharides may affect the biological function and

disposition of antibodies [47]. Kumpel *et al.* reported that the structure of lactosamine affected antibody-dependent cellular cytotoxicity (ADCC), which is a major function of the therapeutic antibodies [48, 49]. The presence of bisecting GlcNAc has also been reported to enhance the ADCC activity [50,51]. Furthermore, recent reports indicated that the absence of the Fuc residue at the innermost GlcNAc of the reducing end showed more clearly ADCC [52, 53]. Therefore, monitoring of oligosaccharide chains expressed in pharmaceutical antibodies is quite important for the quality control in the manufacturing processes.

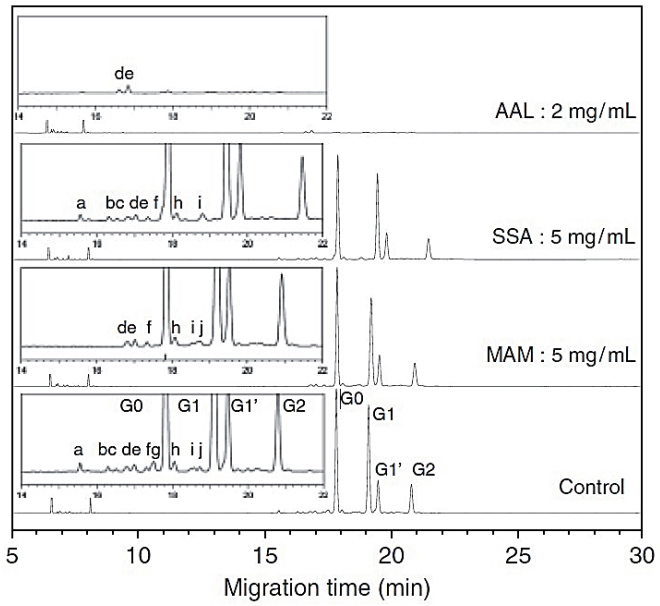

Fig. 13. Partial-filling lectin affinity electrophoresis of APTS-labeled oligosaccharides from rituximab using AAL (2 mg/mL), SSA (5 mg/mL) and MAM (5 mg/mL).

3.1.5.1 PFACE analyses of APTS-labeled oligosaccharides from rituximab

Rituximab is a recombinant antibody used for the treatment of non-Hodgkin's lymphoma [54]. This antibody contains minute amount of high-mannose and hybrid type oligosaccharides [55]. A typical electropherogram for the analysis of APTS-labeled oligosaccharides from rituximab is shown in Fig. 13 (control). APTS-labeled oligosaccharides were observed between 15 and 23 min. We chose three lectins (MAM, SSA and AAL) for a profiling study of antibody-derived oligosaccharides. MAM interacts with the Neu5Acα2-3Gal structure. As shown in Fig. 13, the preinjection of MAM dissipated some minor peaks around 16 and 17.5 min (peaks a, b, c and g). All these peaks also disappeared by digestion with α2,3-neuraminidase (data not shown). Conversely, only two peaks (g and j) disappeared due to the addition of α2,6-linked NeuAc specific SSA. Almost all peaks of rituximab oligosaccharides disappeared by the addition of Fuc-specific AAL. However, two peaks remained at around 17 min, and these peaks also remained during PFACE with ECA. The combination of PFACE using ECA, MAM, SSA and AAL is very useful for the characterization of non-reducing terminal structures in glycoproteins because their structures are associated with ADCC [56], complement-dependent cytotoxicity (CDC) [56, 57] and clearance [58, 59] of therapeutic antibodies.

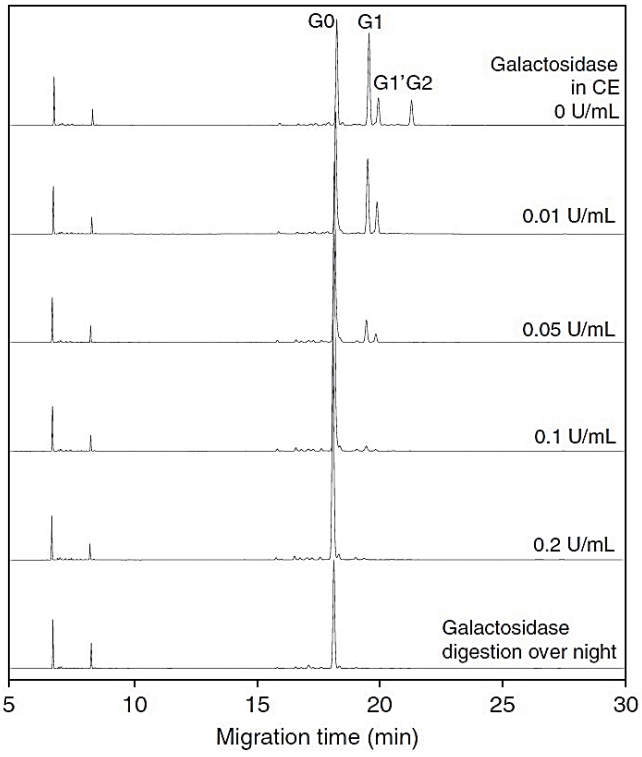

Fig. 14. Electropherogram of APTS-labeled oligosaccharides from rituximab after injection of various concentrations (0–0.2 U/mL) of α-galactosidase.

3.1.5.2 Partial-filling enzymatic digestion and separation of APTS-labeled oligosaccharides

β-Galactosidase hydrolyzes β1,4-linked galactose residues at the non-reducing end of the oligosaccharides. After the introduction of a galactosidase solution (0.2 U/mL), the APTS-labeled oligosaccharides from rituximab were injected and separated. The intensities of peaks corresponding to G1, G1', G2 and some minor peaks having Galβ1-4 structures decreased, and the peak intensity of G0 increased with the increase in galactosidase concentration (Fig. 14). The change in the profile and peak area percentage was comparable with the same oligosaccharides digested in solution overnight at 37ºC (upper trace of Fig. 14). The reaction time while oligosaccharides passed over the enzyme injection plug was estimated to be 3 min from the migration time of oligosaccharides and the length of the enzyme

injection plug in the capillary. The electropherogram of partial-filling digestion with 5 U/mL of neuraminidase in the capillary is shown in Fig. 15. Minor peaks appeared around 17 and 18.5 min (peaks a, b, c and g) were disappeared and the profile was similar to that of PFACE with MAM (Fig. 13). Though these results showed that not all exoglycosidases are suitable for partial-filling enzymatic digestion, a combination of partial-filling techniques using a series of lectins and exoglycosidases could be useful for the characterization of oligosaccharide structure of therapeutic antibodies.

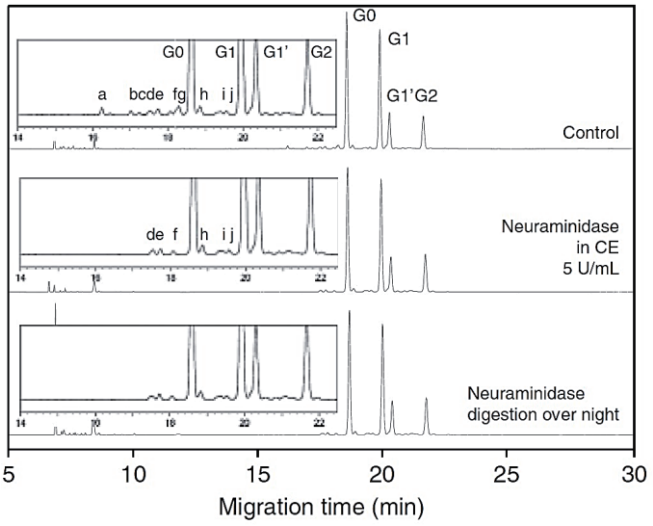

Fig. 15. Electropherogram of partial-filling enzymatic digestion of rituximab-derived oligosaccharides using α-neuraminidase (5 U/mL).

3.1.6. Specific detection of N-glycolylneuraminic acid and Galα1-3Gal epitopes of therapeutic antibodies by partial-filling capillary electrophoresis

3.1.6.1. Specific detection of Neu5Gc residues with anti-Neu5Gc antibody.

Because there are no lectins or enzymes that interact with or hydrolyze Neu5Gc residues specifically, we used anti-Neu5Gc antibody as a chicken polyclonal IgY [60]. After introduction of 2.6 μM anti-Neu5Gc antibody solution to the capillary, the APTS-labeled oligosaccharides from palivizumab were injected and separated. As shown in Fig. 16, small peak appeared at 16.5 min (peak A) was disappeared. Peak A also disappeared after partial-filling enzymatic digestion with α-neuraminidase. These results show that peak A is a glycan with Neu5Gc residues at the non-reducing end. By contrast, no peaks disappeared with pre-injection of anti-Neu5Gc antibody in rituximab [61].

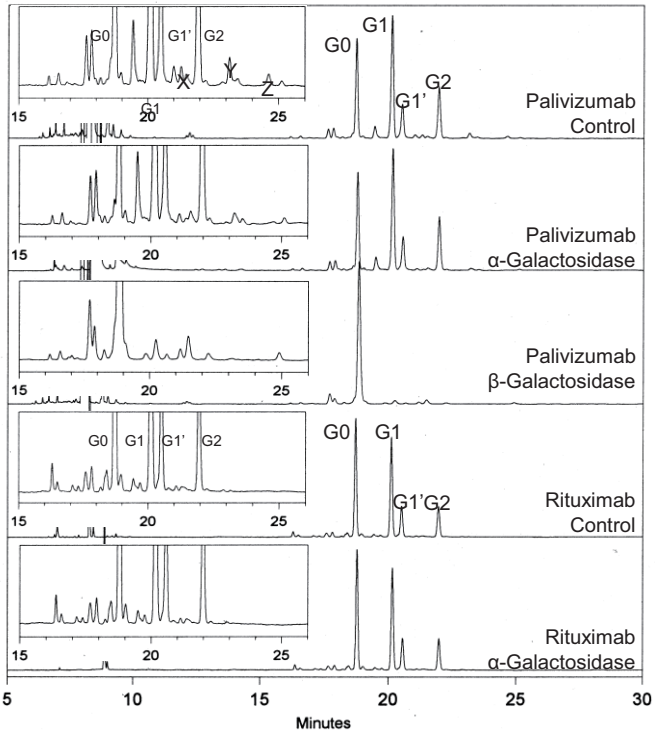

Fig. 16. Partial-filling affinity electrophoresis with anti-Neu5Gc antibody (Ab) and partial filling enzymatic digestion with α-neuraminidase (5 U/ml) of APTS-labeled oligosaccharides from palivizumab and rituximab.

3.1.6.2 Specific detection of α-Gal residues using α-galactosidase.

GSL I-B4 is reported to be specific for terminal α-Gal residues, and have been used to detect the α-Gal epitope in xenotransplantation research [62]. However, when evaluating the specificity of this lectin to porcine thyroglobulin, we surprisingly observed unfamiliar specificity of this lectin, which recognizes mono-sialylated biantennary glycan. Therefore, we chose α-galactosidase for detection of α-Gal residues. After introduction of 75 U/ml α-galactosidase to the capillary, the APTS-labeled oligosaccharides from palivizumab were injected and separated. A minor peak (Z) disappeared, and two peaks (X and Y) decreased in size (Fig. 17). Moreover, in the partial filling enzymatic digestion with β-galactosidase, peak Y disappeared and peak Z did not (Fig .17). This result shows that peak Y has β1,4-linked Gal residues on its non-reducing end and peak Z does not. The glycans migrate in order of increasing size (G0<G1<G2<G2+Hexose, etc.), and it is presumed that peak Y is for G2 with an additional α1,3-linked Gal residue and peak Z is for G2 with two α1,3-linked Gal residues. Although peak X was thought to contain a glycan with α-Gal residues, its structure was not clear.

As shown above the partial-filling CE could be used for detection of two glycan epitopes in pharmaceutical recombinant antibodies. This method makes possible to

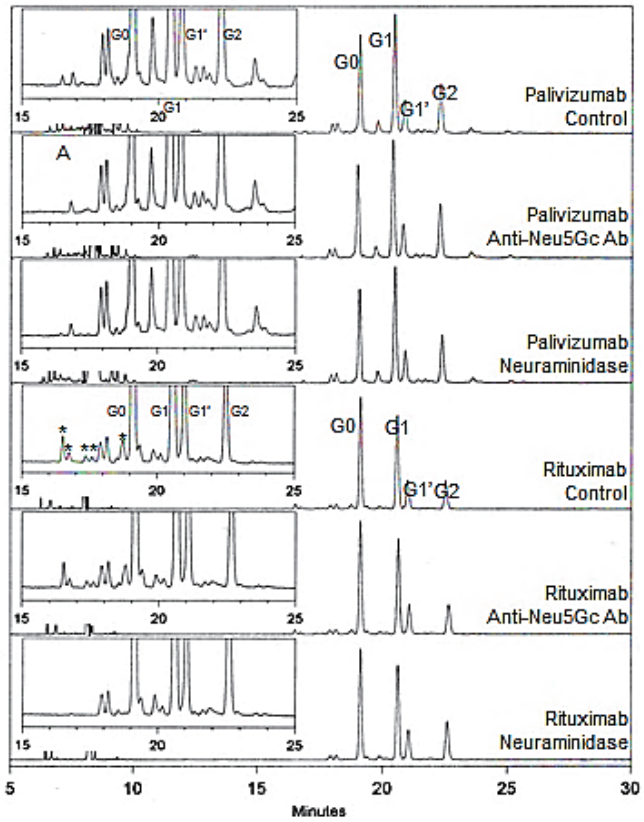

Fig. 17. Partial-filling enzymatic digestion of APTS-labeled glycans from palivizumab and rituximab using α-galactosidase (75 U/ml).

detect and quantify the two antigens on the biopharmaceuticals in the same analytical sequence. Neu5Gc and α-Gal epitopes are the most important modifications, and should be carefully monitored and controlled in manufacturing processes. The simplicity and high sensitivity of this method will be valuable for detection of glycan epitopes during development of biopharmaceutical manufacturing process.

4. *In situ* fabricated polyacrylamide-based preconcentrator gels for microchip electrophoresis of oligosaccharides [63,64]

4.1. Sulfonate-type polyacrylamide gel on a simple poly(methyl methacrylate) microfluidic chip for permselective preconcentration and capillary electrophoresis of anionic saccharide derivatives

On-chip mode capillary electrophoresis has been the subject of extensive research over the past decade [65,66]. Translation of CE methods from traditional capillary systems to a microchip platform provides advantages including rapid separation and easy quantitation of sample components. However, microfluidic devices can process picoliter to nanoliter quantities of sample delivered from the sample reservoir with a few μL volume of sample reservoirs, therefore the concentration of sample often fall below the detection threshold of the analytical systems. Sample solutions are introduced to microfluidic systems by electrokinetic injection, which often causes selective injection and induces overestimation of analytes with higher electrophoretic mobilities, which spoils the analytical use of this method.

One promising alternative to overcome scaling problem is online sample preconcentration which enables the concentration of all analytes to the separation channel. Fabrication of an anionic preconcentrator on a commercial cross-channel chip based on the in-capillary photopolymerization was applied to the sensitive analyses of APTS-labeled oligosaccharides.

4.1.1 Fabrication of anionic preconcentrator on a cross-channel type microchip

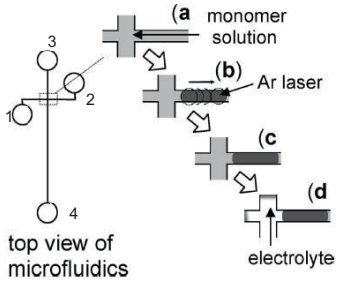

Fig. 18. Schematic illustration of fabrication, by photopolymerization, of polyacrylamide preconcentration gel with a pore size compatible to the electrical double layer.

Photopolymerization of an anionic polyacrylamide layer was achieved at a sample waste channel near the channel cross by irradiation of an argon ion laser, as portrayed in Fig. 18. At first, all channels were filled with a monomer solution comprised of acrylamide, *bis*-acrylamide, acrylamidesulfonic acid, and riboflavin as photoinitiator; then a laser beam with ~100-μm beam radius was irradiated to channel 2 at positions of 100-600 μm from the channel cross by handling the sample stage of the microscope. The unwanted nonpolymerized gel solution was removed and displaced with buffer solution by pumping it from reservoir 4. Finally, reservoir 1 was filled with anionic sample solution; then the voltage was applied to reservoir 2 with 50-200 V and to reservoir 1 for ground. The concentration of anionic sample components started at the interface of the cathodic side of the gel layer. Anionic fluorescent reagent such as APTS or fluorescein moved immediately to the channel cross, and the concentration was continued and reached a plateau within 5 min.

Preconcentrations using ionic nanosized filters are called permselective concentration [67]: Negatively charged

nanofluidic filters made of PDMS or glass cause the anion exclusition, and the overall ion concentration will be decreased on the cathodic side because of the concentration polarization effect. The ion depletion thickens the Debye layer and makes it overlap considerably in the nanofluidic channel, which hastens the concentration polarization. Therefore, above a certain threshold value of voltage, anions such as biomolecules are prohibited from penetration because of their repulsion to negative potential [68]. At the interface, anionic samples coming from the sample reservoir can be trapped continuously and collected. The preconcentration of proteins reportedly proceeds almost linearly with the time of voltage application; the preconcentration efficiency is very high, reaching almost 1 million-fold.

We used a PMMA-made microchip that had been neutrally coated with a blocking reagent and to which had been added neutral polymers such as hydroxypropylcellulose to the background electrolytes, which renders electroosmosis negligible. This suppresses the generation of EOF in the channel and simplifies the preconcentration process. A strong negative charge of sulfonate groups incorporated in the polyacrylamide gel layer acts to disturb anions to permeate to the gel layer. In contrast, cationic substances could be repeatedly adsorbed and desorbed by ion-exchange effect and preferentially travel across the anionic gels.

4.1.2. Factors affecting preconcentration of anions

The concentration and molar ratio of acrylamide/*bis*-acrylamide determines the mechanical strength and pore size of the nanofluidic filter. Sufficient mechanical strength was obtained at a concentration of more than 20%T and 15%C, at which we were unable to observe any breakage. The permselective concentration was observed at more than 4% 2-acrylamide-2-methylpropanesulfonic acid. However, the higher concentration of sulfonate decreases the polymerization rate. Based on those results, we chose the 16.7% acrylamide, 5.3% *bis*-acrylamide and 3.9% 2-acrylamide-2-methylpropanesulfoic acid as the monomer concentration, which corresponds 25.9%T, 20%C, and 5.9% sulfonic acid. The pore size of this acrylamide gel is unknown. However, the respective pore sizes of 4.6%T/1.5%C and 10.5%T/10%C polyacrylamide gels are reportedly 142 and 19 nm [69]. Therefore, the pore size of the gel used for the study described herein is estimated as less than 10 nm, which is sufficient to obtain permselectivity.

Buffer components and their concentration also influence the efficiency and time for the preconcentration of anions. It is noteworthy that the preconcentration depended on the anionic dissociation strength of the sample and buffer used. In the borate or acetate buffer system, both APTS and fluorescein can be concentrated at the preconcentrator gel interface; however, fluorescein cannot be concentrated in a phosphate buffer system. Moreover, the start of APTS preconcentration is severely delayed in phosphate buffer: it takes ~10 min to reach the anionic gel boundary. This phenomenon might be explainable by isoelectric focusing of anions, and the efficiency of concentration depends on the *K*a of sample components and anions in background electrolytes.

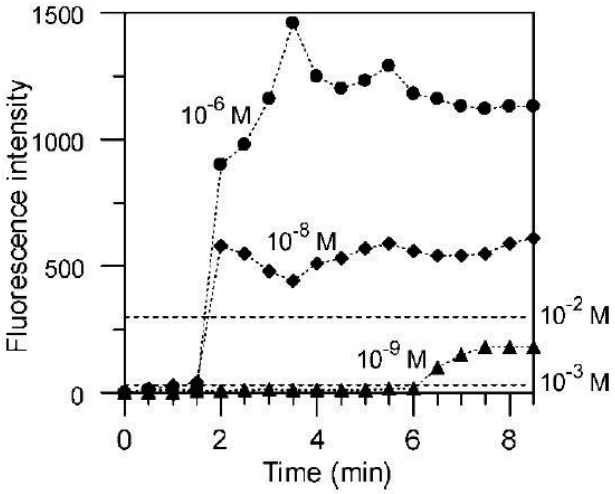

Fig. 19. Time course of the concentration of APTS. Concentration of each sample is observed at the fluorescence intensities at the channel cross, which is depicted as a dotted line. Broken lines indicate the average fluorescence intensity of each concentration at the channel cross without fabrication of the photopolymerized gel.

The preconcentration of APTS was examined at the concentration between 10^{-6} and 10^{-9} M by observing the fluorescence intensity at the channel cross (Fig.19). The relation between the concentration and fluorescence intensity at the steady state is shown as broken lines. As presented in the solid curves of Fig. 19, the increase of fluorescence intensity of APTS started at 1.5 min at a concentration more than 10^{-8} M; it showed a convex curve until 2 min and reached a plateau. The concentration of 10^{-9} M APTS is apparently retarded thereafter and requires 6 min for the initiation of concentration. The detection limit of APTS were ~10^{-9} and 10^{-4} M with and without the presence of a preconcentrator, respectively. Therefore, the preconcentration efficiency of this method was calculated to be 100 000-fold. The volume of the channel cross of the microchip was calculated as 300 pL; the sample chamber has the volume of 10 μL. Therefore their volume ratio was ~1:33000. Consequently, most of the sample anions added to the sample chamber were moved and concentrated at the gel boundary.

4.1.3. Application to the analyses of APTS-labeled oligosaccharides

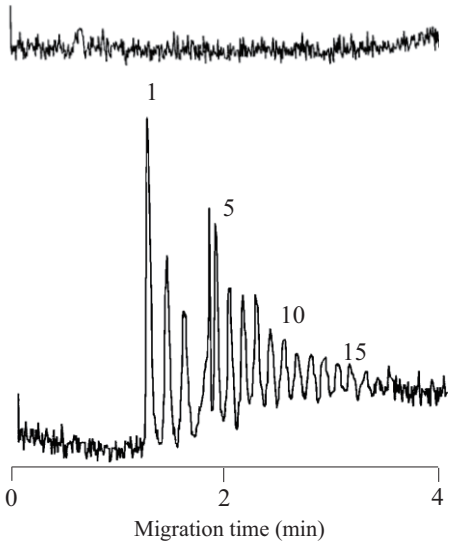

Fig. 20. Preconcentration and electrophoretic separation of APTS labeled isomaltooligosaccharide mixture under the optimized conditions (lower trace) and the reference (upper trace).

In the application of permselective preconcentration to the microchip electrophoresis of some FITC-labeled glycoconjugate analysis, we observed three unexpected phenomena: (1) decrease of migration time, (2) lower concentration factor expected from the observation at channel cross, and (3) high preconcentration in slow migration components (data not shown). Considerable improvement was achieved using a sample solution poured to reservoir 3 and concentrated by applying voltage to reservoir 2, as shown in Fig. 18, and then applied 1 kV on reservoir 4 and connected to reservoir 2 to ground for separation of APTS-oligosaccharides. Among the four channels, only channel 2 causes no diffusion because of the presence of the preconcentrator gel. This will suppress unwanted diffusion of peaks. The lower trace of Fig. 20 portrays the separation of the APTS-labeled isomaltooligosaccharide mixture (10^{-8} M in total) under these potential settings. No decrease of migration times was observed in this case. Moreover, higher oligosaccharides with d.p. greater than 15 were also observed in this separation. Therefore, the oligosaccharides with longer migration time are also concentrated with high efficiency. The separation of the same sample without using the preconcentrator gel is also depicted in upper trace of Fig. 20. Concentration of these saccharides corresponds to less than the detection threshold. Preconcentration factors were calculated to be more than 20 000. These two figures show that our method is an extremely efficient concentration method.

The ionic polyacrylamide gel can be fabricated by introducing an acrylamide solution into a microchannel, with subsequent polymerization by irradiation with an argon laser beam of ~100-μm diameter for a few minutes at a sample waste channel near the cross. The resultant ionic gel preconcentrator has sufficient mechanical strength. The preconcentrator trapped efficiently ionic analytes possessing opposite charge in the front of the nanofilter with application of ~100 V between the sample and sample waste reservoirs for a few minutes; the analyte was then introduced into the separation channel using the gated injection method. This method enables 10^5-fold concentration. This method could be applied to the analyses of APTS derivatives of oligosaccharides

4.2. Microchip electrophoresis of oligosaccharides using lectin-immobilized preconcentrator gels fabricated by in situ photopolymerization [70]

As described in Section 3, the high specificity of lectins against certain oligosaccharides is helpful for profiling in glycoproteomics analysis. Lectin affinity capillary electrophoresis [71-73] and lectin microarrays [74-76] have been proposed for this purpose. Affinity columns immobilized with various lectins are useful for sorting complex mixtures of oligosaccharides based on their structural differences [77]. A silica column with a mixture of immobilized lectins was proposed for enrichment of glycans on the microscale, and the procedure was combined with nano-LC-MS/MS to identify numerous glycopeptides [78]. Unique lectin applications include in a monolithic affinity column fabricated in the channel of a microfluidic chip for separation of three types of glycoprotein [79].

A lectin-impregnated polyacrylamide gel would have many advantages over other affinity materials. Lectin-immobilized gels with various specificities can be prepared by a common, single step procedure without modification of the lectin, and the concentration of the lectin is easily optimized by changing the quantity in the acrylamide solution. Recovery and separation of captured oligosaccharides can be attained by lowering the pH of the electrolyte for denaturation of the lectin [80,81].

A lectin-impregnated gel was fabricated at the channel crossing point using *in situ* photopolymerization by irradiation with an argon laser. The saccharides in a sample solution were specifically and continuously trapped in the lectin gel by applying a voltage across the gel plug. The entrapped sample was released from the gel by delivery of acidic phosphate ions to the gel. The broad sample band obtained was effectively concentrated by transient isotachophoresis, which involved passing the sample through a pH gradient generated by a highly concentrated alkaline buffer phase that was delivered from the anodic end of the separation channel. This device was applied to sensitive analysis of glycoprotein-derived oligosaccharides.

4.2.1 Mechanisms for in situ photopolymerization of lectin gel and preconcentration of oligosaccharides

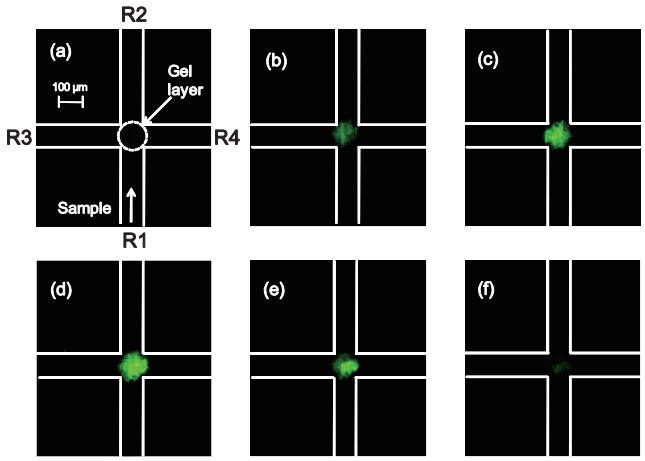

Fig. 21. Time-course of the concentration and the release of APTS derivatives of mannobiose at the channel crossing point in the Con A-impregnated polyacrylamide gel. All the channels were filled with 25 mM Tris/acetate buffer (pH 7.0); the left chamber (R3) was filled with 25 mM Tris/phosphate buffer (pH 2.0); the right chamber (R4) was filled with 200 mM sodium borate buffer (pH 11.0); the lower chamber (R1) was filled with 10^{-6} M APTS-mannobiose, and 150 V was applied between R1 and R2 for 0 s (a), 30 s (b), 90 s (c), and 180 s (d). Then voltage settings were changed to 200, 200, 0, and 800 V for R1, R2, R3, and R4, respectively. Images (e) and (f) show the decrease in the fluorescence of APTS-mannobiose after 10 and 15 s.

A method was developed to capture and concentrate specific saccharides in a sample mixture onto a lectin-impregnated polyacrylamide gel, with subsequent separation and detection on a microfluidic chip. Fig. 21 shows images at channel crossing point for this method with APTS-mannobiose and Con A-impregnated gel as a model system. A Con A-containing acrylamide solution was delivered to the channels from R2 under pressure. A round Con A-impregnated gel was fabricated at the intersection of the channels by irradiation argon laser beam. This step is referred to as the affinity matrix fabrication step. After washing the channels with neutral buffer, R1 to R4 was filled with APTS-mannobiose, neutral buffer, acidic buffer, and basic buffer, respectively. When voltage was applied from R1 to R2, the fluorescence intensity at the lectin plug gradually increased and finally reached saturation (Fig. 21(b)-(d)). This indicates APTS-mannobiose trapped in the Con A plug (saccharide concentration step). Then an electric field was applied across R3 and R4. After 10 s, the concentrated APTS-mannobiose was released from the gel to the separation channel as a relatively broad band (elution step). The sample components were finally stacked at the boundary of phosphate-acetate ion in a pH gradient generated by a large amount of sodium ion delivered from the anode. The stacked sample was separated and detected at the end of channel 4 (separation and detection step).

In the fabrication of an affinity matrix, lectin should be effectively immobilized and sustain its activity without leakage using a 20%T/20%C gel. Green fluorescent riboflavin was chosen as the photoinitiator for gel fabrication. A voltage (500 V) was then applied between reservoirs R1 and R2 for 3 min to remove any riboflavin remaining in the lectin-immobilized gel before analysis. The concentration factor of an oligosaccharide with this method will be limited by the amount of lectin immobilized in the gel.

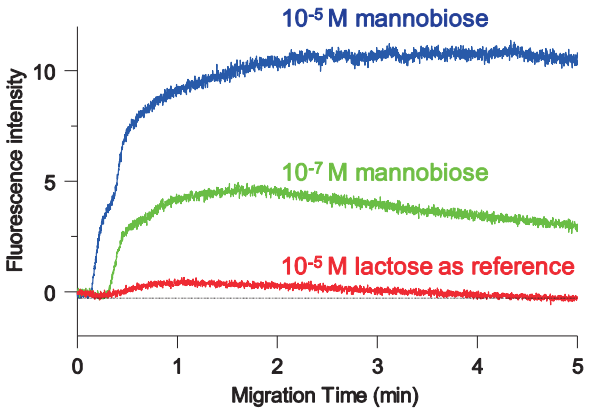

Fig. 22. Time course of the changes in the fluorescence intensity due to trapping of APTS-mannobiose on the Con A-impregnated gel formed at the channel crossing point. The concentrations of APTS mannobiose are indicated on each plot. The red line indicates the fluorescence intensity of 10-5 M APTS-lactose as the reference.

Fig. 22 shows the time-course of the change of the fluorescence intensity of APTS-mannobiose (10^{-5} M and 10^{-7} M) at the Con A-immobilized gel. We also measured the fluorescence intensity of 10^{-5} M APTS-lactose at the gel as the reference. APTS-lactose indicates a profile whose fluorescence intensity reached maximum at *ca.* 50 s, then linearly decreased and reached zero after 4 min. The same fluorescence profile was also observed at the channel cross of the same microchip without fabricating lectin gels. In contrast, affinity entrapment of APTS-mannobiose increased until 40 s, and reached a plateau at >2 min. The fluorescence of 10^{-5} M APTS-mannobiose at the Con A-immobilized gel increased approximately 20 times of 10^{-5} M APTS-lactose by 2 min. The fluorescence of 10^{-7} M APTS-mannobiose was 8.8 times more intense than that of 10^{-5} M APTS-lactose. This implies that the concentration factor of this method is *ca.* 800 times. The binding constant of mannose is not so strong, and indicates around 7 000 M^{-1} [82]. Therefore, the low amount of APTS-mannobiose bound to the Con A-impregnated gel should be due to the dynamic binding equilibrium between APTS-mannobiose and Con A. By

contrast, most glycoprotein-derived oligosaccharides have strong binding affinities of $>10^6$ M^{-1} [83,84]. Higher concentrations of lectin may enhance the trapping capability.

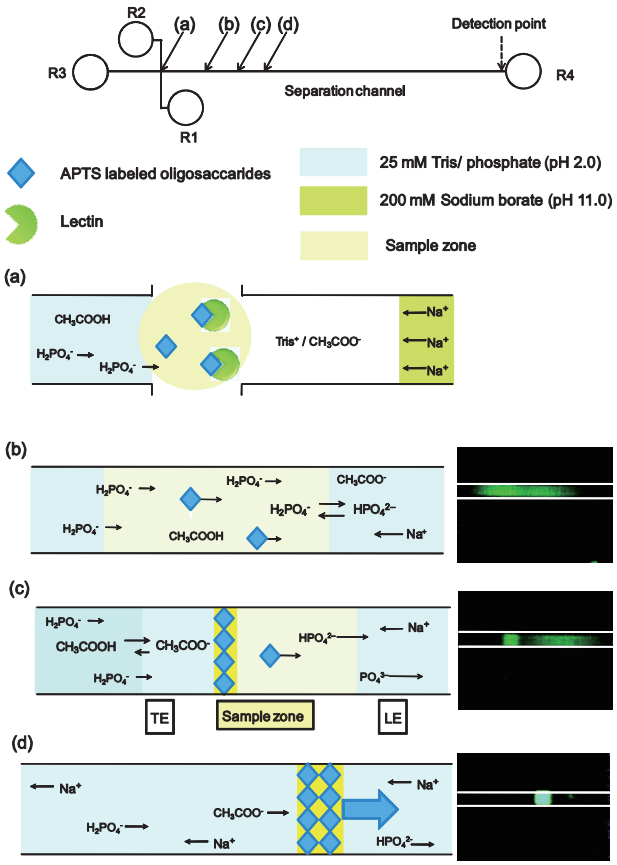

Fig. 23. Schematic diagram of a microchip, and illustrations and fluorescent images ((a)–(d)) of the sample band moving and stacking in the separation channel. The solid arrows indicate the positions where the fluorescent images were obtained, and broken arrow indicates the point of laser-induced fluorometric detection.

Denaturation of the lectin by altering the pH is one of the most promising methods for rapid release of oligosaccharides from lectin-impregnated gels. As shown in Fig. 21(e) and (f), APTS-mannobiose was released from the gel by delivering acidic buffer. It began at 10 s and was almost complete at 15 s. Slow elution produced a sample band of about 400 μm in length. Transient isotachophoresis stacking was chosen for concentration of the sample band. APTS saccharides were eluted with phosphate ions to Tris/acetate buffer. The sample band contained acetate and phosphate as co-ions in the pH gradient. In the sample band, the phosphate ion migrated faster than the APTS-saccharides, and acetic acid almost lost its charge in the presence of the phosphate ion. Sodium borate buffer (200 mM, pH 11.0) was used as the anolyte. The sodium ions were quickly and continuously delivered to the cathode in the separation channel in the opposite direction to the sample flow. This formed a pH gradient at the front of the sodium ion band, where monovalent, and some bivalent phosphate ions could be converted to bivalent and trivalent phosphate ions, which increased their electrophoretic mobility and function as the leading electrolytes. By contrast, acetic acid is partially ionized in the pH gradient and acts as the terminal electrolyte for stacking of the APTS-oligosaccharides. When the sample band met the boundary of the concentrated sodium ion delivered from the anode (Fig. 23(a and b)), the sample band was concentrated from the back and formed a leading shape (Fig. 23(c)), and finally formed a concentrated sharp band (Fig. 23(d)). Then the sample components were separated in this concentrated sodium phosphate phase and finally detected at the end of the separation channel. The entrapment efficiency calculated from the concentration and the peak areas was 460 times that of the pinched injection method. The separation efficiency was 6800 theoretical plates compared with 3600 plates for the pinched injection method (data not shown).

4.2.3 Application to the analysis of glycoprotein-derived oligosaccharides

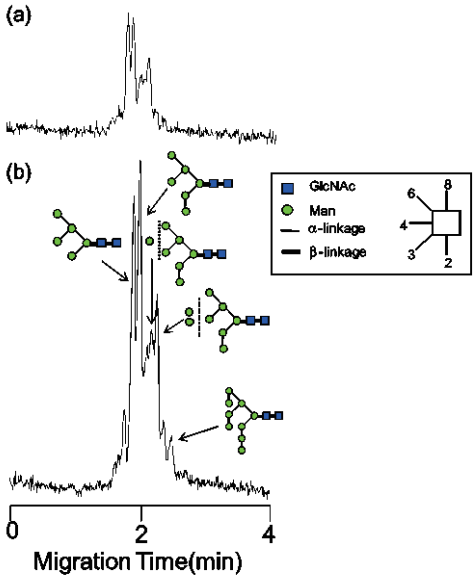

Fig. 24. Electrophoretic separation of preconcentrated APTS glycans derived from bovine ribonuclease B with preconcentration by Con A-impregnated gel (b) and the 50 times more concentrated sample analyzed by pinch injection without preconcentration (a).

Bovine ribonuclease B contains a series of high-mannose-type oligosaccharides consisting of five to nine mannose residues with a di-*N*-acetylchitobiose core. Con A was chosen to trap these high-mannose type oligosaccharides (Fig. 24). A solution of oligosaccharides (5×10^{-8} M, corresponding to 70 μg/L of this glycoprotein) was delivered to the gel. Ribonuclease B-derived oligosaccharides had

signals about two to three times more intense than those obtained by the pinched injection of 50 times more concentrated sample. Therefore, the oligosaccharides were concentrated approximately 150 times. The resolution of this method was almost the same as that obtained by the pinched injection method.

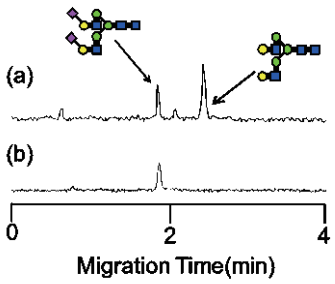

Fig. 25. Separation of a 1 : 2 mixture of sialylated and asialylated glycans derived from human transferrin preconcentrated with a SSA impregnated gel (b) and the 25 times more concentrated sample analyzed by pinched injection without preconcentration (a).

The lectin-immobilized gel method enables specific entrapment and concentration of oligosaccharides. α2,6-Linked neuraminic acid specific lectin, SSA was immobilized to the gel, and a 2:1 mixture of asialo- and sialo-oligosaccharides derived from transferrin was delivered to the SSA gel for 5 min at a concentration of 60 nM. Analysis by pinched injection of the mixture of asialo- and sialo-oligosaccharides produced peaks at 0.6 min for APTS, 1.9 min for disialylated oligosaccharides, 2.4 min for asialooligosaccharides as shown in Fig. 25(a), and unknown small peak at 2.1 min. By contrast, analysis using SSA lectin produced only one signal for the NeuAc containing oligosaccharide at 1.9 min (Fig. 25(b)). These results show this method is effective for trapping specific glycans in complex oligosaccharide mixtures.

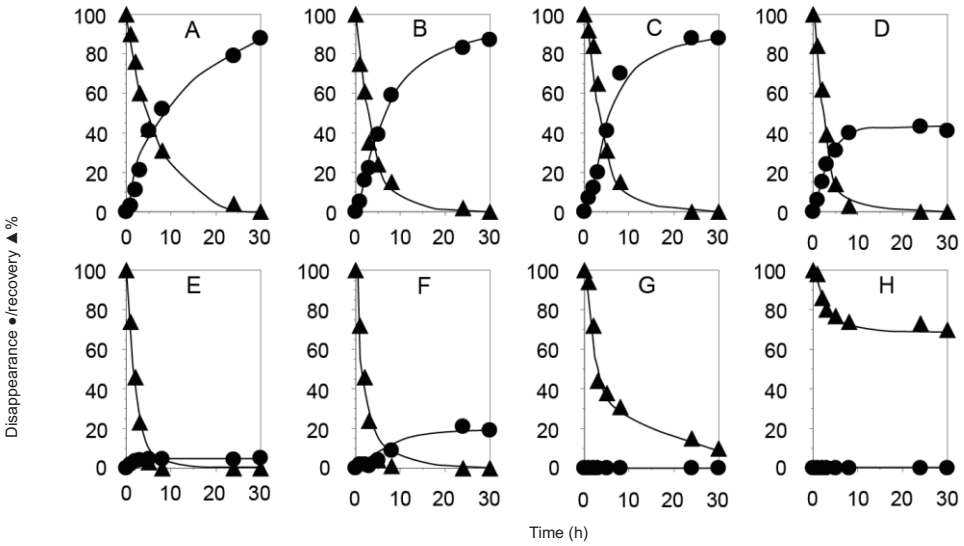

Fig. 26. Time course of the disappearance rate of maltose derivatives (●) and recovery of free maltose (▲) by incubating 50 µl of 0.1mM concentration of maltose derivative with each 5 µl of hydrogen peroxide and acetic acid at 30° C: (A) p-ABEE; (B) p-ABN; (C) AMC; (D) o-ABA; (E) o-ABAD; (F) o-ABN; (G) ANTS; (H) AP.

5. Recovery of free oligosaccharides from derivatives labeled by reductive amination [85]

Glycans released chemically or enzymatically from the protein core are frequently labeled with various aromatic primary amines such as 2-aminobenzamide (o-ABAD) [86], 2-aminobenzoic acid (o-ABA) [87], 2-aminoacridone [88], 2-aminopyridine (AP) [89], 7-amino-4-methylcoumarin (AMC) [14], and 8-aminonaphthalene-1,3,6-trisulfonate (ANTS) [90]. The glycans are converted to their fluorescent 1-aminoalditol derivatives by a common reaction called reductive amination in the presence of borohydride reagents. However, it is difficult to use the labeled glycans for functional studies because the introduction of labeling groups causing open-ring structure of the terminal *N*-acetylglucosamine and lost of aldehyde group. Therefore the subsequent modification to neoglycoprotein, or immobilization onto affinity matrix, usually is difficult.

Kallin and coworkers reported that 1-aminoalditol derivatives prepared by reductive amination with 4-trifluoroacetamidoaniline [91] is convertible to parent-free saccharides through treatment with an acidic hydrogen peroxide solution [92]. Recoveries of free saccharides were 66 –83%. This study explores a method for recovery of free saccharides from various types of 1-aminoalditol derivatives.

5.1. Specificity of the reaction conditions

Maltose derivatives of *p*-ABEE, *o*-ABN, *p*-ABN, AMC, *o*-ABA, *o*-ABAD, AP, and ANTS were used to examine the recoveries of free maltose from these derivatives by hydrogen peroxide oxidation. This reaction proceeded under the presence of acid, and the yield of maltose depended strongly on the type of acid used. The reaction proceeded

slowly in the solutions, including formic acid, hydrochloric acid, and nitric acid. In contrast, higher recoveries were obtained using sulfuric acid and acetic acid, but sulfuric acid is difficult to remove from the reaction mixture. Therefore, we chose acetic acid for this reaction. Fig. 26 shows time course of the recoveries of maltose from the derivatives. With the progress of the reaction, starting materials were decreased gradually (closed triangles for all compounds), and recovered free maltose analyzed after labeling with PMP (closed circles) was increased. Derivatives of *p*-ABEE, *p*-ABN, and AMC showed good recoveries of free maltose in the yields of 87, 88, and 90%, respectively, after 30 h. Although *o*-substituted aniline derivatives (*o*-ABA, *o*-ABAD, and *o*-ABN) were decreased more rapidly than the derivatives of *p*-ABEE, *p*-ABN, and AMC, maltose recoveries from the o-substituted aniline derivatives were 5 – 40%. These results indicated that the hydrogen peroxide reaction of the *o*-aniline derivatives accompanied the formation of by-products. Fig. 26G and H show results obtained for ANTS and AP derivatives, respectively. Both derivatives were resistant to this reaction; they could not be completely eradicated even after 30 h incubation. Furthermore, only negligible amounts of maltose were detectable from these two derivatives.

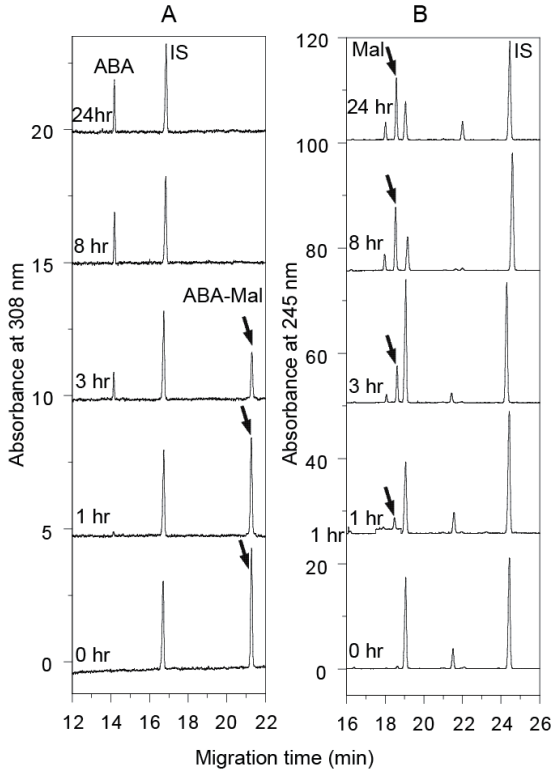

Fig. 27. Selected electropherograms of hydrogen peroxide-treated o-ABA maltose (A) and free maltose as its 1-phenyl-3-methyl-5-pyrazolone derivative (B) in reaction with hydrogen peroxide/acetic acid.

Low recovery of maltose from *o*-substituted aniline derivatives suggested the formation of by-products during reaction with hydrogen peroxide. Fig. 27 shows electropherograms during the time course study of *o*-ABA maltose. The maximum yield of maltose recovered from *o*-ABA derivatives was approximately 40%. Peaks of *o*-ABA-labeled maltose that appeared at 21min (Fig. 27A) decreased gradually with the progress of reaction and disappeared completely after 8 h. In conjunction with *o*-ABA maltose disappearance, free maltose as PMP derivative appeared at 18.7min in Fig. 27B. Both separations were performed using alkaline borate buffer. Therefore, all analytes were forced to the cathodic end *via* detection by fast electroendoosmotic flow. We were able to observe only those peaks of removed

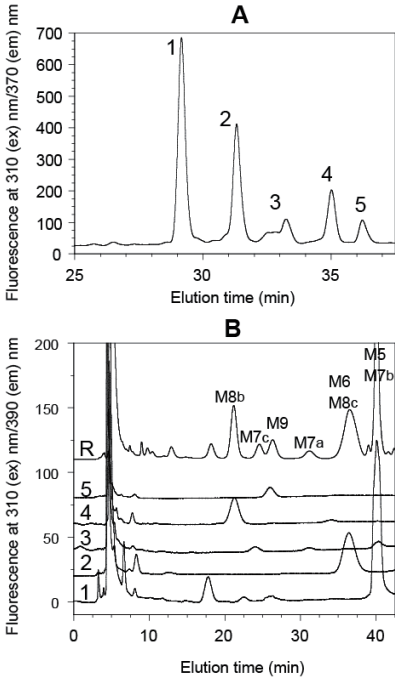

M5 Manα1-6Manα1-3Manα1↘6Manα1↗3Manβ1-4GlcNAcβ1-4GlcNAc

M6 Manα1-6Manα1-3Manα1↘6Manβ1-4GlcNAcβ1-4GlcNAc
Manα1-2Manα1↗3

M7a Manα1-6Manα1-3Manα1↘6Manβ1-4GlcNAcβ1-4GlcNAc
Manα1-2Manα1-2Manα1↗3

M7b Manα1-6Manα1-2Manα1-3Manα1↘6Manβ1-4GlcNAcβ1-4GlcNAc
Manα1-2Manα1↗3

M7c Manα1-2Manα1-6Manα1↘6Manβ1-4GlcNAcβ1-4GlcNAc
Manα1-3
Manα1-2Manα1↗3

M8b Manα1-2Manα1-6Manα1↘6Manβ1-4GlcNAcβ1-4GlcNAc
Manα1-3
Manα1-2Manα1-2Manα1↗3

M8c Manα1-6Manα1↘6Manβ1-4GlcNAcβ1-4GlcNAc
Manα1-2Manα1-3
Manα1-2Manα1-2Manα1↗3

M9 Manα1-2Manα1-6Manα1↘6Manβ1-4GlcNAcβ1-4GlcNAc
Manα1-2Manα1-3
Manα1-2Manα1-2Manα1↗3

Fig. 28. HPLC fraction 1-5 of ribonuclease B glycans as their *p*-ABEE derivatives on an Amide80 column (A) and separation of fractionated glycans as AP derivatives *via* free glycans on an ODS column (B). Numbers in panel B indicate fraction numbers on the amide column (A), and R is the reference data of AP glycans directly derived from ribonuclease B.

o-ABA and *o*-ABA maltose in Fig. 27A, and free maltose as a PMP derivative.

5.2. Application to p-ABEE derivatives of glycoprotein glycans

The reaction was applied to peak identifications of *p*-ABEE derivatives of glycans derived from some glycoproteins. Bovine pancreas ribonuclease B contains a series of high mannose type glycans, $Man_{5\text{-}9}GlcNAc_2$, and contains positional isomers of outermost mannose residues in $Man_7GlcNAc_2$ and $Man_8GlcNAc_2$. High mannose-type glycans were separated based on linkage type were separable on an ODS column. The *p*-ABEE derivatives of these glycoprotein glycans yielded five peaks on an Amide 80 column, as shown in Fig. 28A. Each peak was fractionated, deionized, and treated with hydrogen peroxide and subsequently labeled with AP. Fig. 28B shows that all fractionated AP glycans gave single peaks on an amide column but that some fractions gave a number of peaks on an ODS column. Fractions 1, 2, and 5 gave single peaks on each chromatogram and are designated as M5, M6, and M9, respectively. Fraction 3 gave three peaks corresponding to three isomers of $Man_7GlcNAc_2$: M7c, M7a, and M7b in the elution order. In contrast, fraction 4 gave mainly only one peak assignable to M8b. Results obtained on $Man_7GlcNAc_2$ and $Man_8GlcNAc_2$ are interesting with respect to the trimming in the biosynthetic pathway of high-mannose-type glycans. Recoveries of glycans as AP derivatives were calculated as 51% for M6, 29% for M7c, and 49% for M8b.

Another application to analysis of sialoglycans derived from human serum transferrin. A weak anion exchange column was used for the separation of ABEE-labeled sialoglycans from transferrin (Fig. 29A). Treatment of these two peaks of ABEE glycans with hydrogen peroxide and following AP derivatization gave peaks at 45 and 50 min on an ODS column as shown in Fig. 29B. Their eluting positions were the same as those obtained on AP labeled glycans derived from transferrin. The conversion recovery was approximately 35%. This result clearly indicates that this reaction conditions are safe for the sialylated glycans.

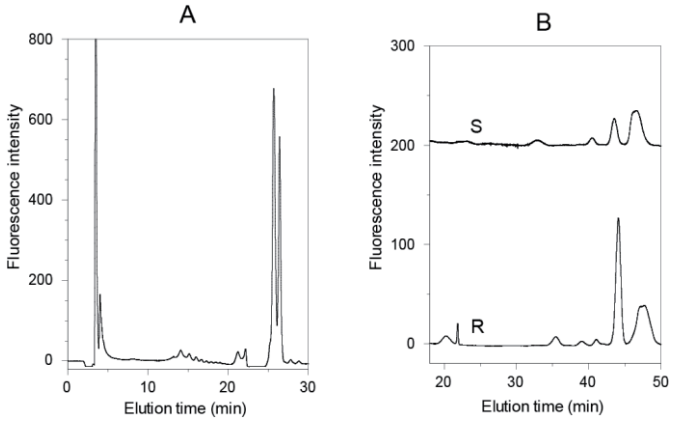

Fig. 29. HPLC analysis of human transferrin glycans as their p-ABEE derivatives on a DEAE-5PW column (A) and separation of their glycans as AP derivatives via free glycans on an ODS column (B, upper trace). R is separation of AP-labeled glycans derived from transferrin as a reference.

5.3. Conversion of AP derivatives to free saccharides

AP derivatives were not convertible to free saccharides. High resistance of AP derivatives to hydrogen peroxide treatment seems to result from the imino function of the pyridine ring, which may stabilize the amino group conjugated with carbohydrate chains from oxidative cleavage. Cyanogen bromide often is used as a blocking reagent of nitrogen atom of pyridine ring by forming pyridinium cyanide. AP maltose was treated with cyanogen bromide for 2 h at 50°C. The reaction products were convertible to free maltose by hydrogen peroxide treatment. The method was applied to conversion of AP-labeled glycans of transferrin, and the recovery was *ca.* 50%.

6. Conclusion

Our recent works concerned on the analysis of glycoprotein glycans were introduced. PNGase F/NBD-F method comprises the digestion with PNGase F for releasing oligosaccharides from glycoproteins and subsequent fluorescent derivatization with NBD-F. Subfemtomole analyses of *N*-linked oligosaccharide with easy operations were attained in a one-pot reaction for about 2 h.

A combination of AMC labeling with neutrally coated capillary enables capillary electrophoretic analysis of reductively aminated saccharides without removal of excess reagents. The method was applied to monosaccharides analysis and oligosaccharide analysis of some glycoprotein specimens.

Partial-filling lectin ACE can be used effectively to study the interaction between glycoprotein oligosaccharides with some plant lectins. Changes in electrophoretic profiles were observed as mobility shift, peak broadening, and peak disappearance. Sequential injection of a suitable set of lectins may enables detection and quantitation of specific oligosaccharides. The LVSEP-PFACE method can be used effectively to study the interaction between minor components of glycoprotein oligosaccharides with some plant lectins with high sensitivity. The method was applied to IgG glycans and found effective in the determination of immunogenic glycans containing terminal NeuGc and α-Gal residues.

In situ photopolymerization of ionic polyacrylamide gel act as the permselective preconcentrator trapped efficiently ionic analytes possessing opposite charge in the front of the nanofilter. This method enables 10^5-fold concentration, and could be applied to the analyses of APTS derivatives of oligosaccharides. The lectin-immobilized gel trapped specific oligosaccharides efficiently with application of voltage for a few minutes, and the method enabled the analysis of a few nM oligosaccharides with high sensitivity. Careful choice of the electrophoretic buffer system for transient isotachophoresis stacking enabled specific detection without the loss of resolution efficiency.

These methods will be helpful in the quality control of glycoproteinaceous pharmaceuticals, and functional studies of glycoprotein glycans.

References

[1] Apweiler, R.; Hermjakob H.; Sharon, N. *Biochim. Biophys. Acta,* **1999**, *1473*, 4-8. DOI: 10.1016/S0304-4165(99)00165-8

[2] Dennis, J. W.; Granovsky, M.; Warren, C. E. *Bioessays,* **1999**, *21*, 412-421. DOI: 10.1002/(SICI)1521-1878(199905)21:5<412::AID-BIES8>3.0.CO;2-5

[3] Varki, R. C. A.; Esko, J.; Freeze, H.; Hart, G.; Marth, J. Essentials of Glycobiology; Cold Spring Harber Laboratory Press, New York, **1999**.

[4] Dube, D. H.; Bertozzi, C. R. *Nat. Rev. Drug Discov.*, **2005**, *4*, 477-488. DOI: 10.1038/nrd1751

[5] Fuster M. M.; Esko, J. D. *Nat Rev Cancer,* **2005**, *5*, 526-542. DOI: 10.1038/nrc1649

[6] Oyama, T.; Yodoshi, M.; Yamane, A.; Kakehi, K.; Hayakawa, T.; Suzuki, S. *J. Chromatogr. B*, **2011,** *879*, 2928-2934. DOI: 10.1016/j.jchromb.2011.08.026

[7] Takahashi, N.; Nakagawa, H.; Fujikawa, K.; Kawamura, Y.; Tomiya, N. *Anal. Biochem.* **1995**, *226,* 139-146. DOI: 10.1006/abio.1995.1201

[8] Isbell, H. S.; Frush, H. L. *J. Am. Chem. Soc.* **1950**, *72*, 1043.

[9] Koller, A.; Khandurina, J.; Li, J.; Kreps, J.; Schieltz, D.; Guttman, A. *Electrophoresis* **2004**, *25*, 2003-2009. DOI: 10.1016/S0304-4165(99)00165-8

[10] Yodoshi, M.; Ikeda, N.; Yamaguchi, N.; Nagata, M.; Nishida, N.; Kakehi, K.; Hayakawa, T.; Suzuki, S. *Electrophoresis*, **2013,** *34,* 3198-3205. DOI: 10.1002/elps.201200612

[11] Anumula, K. R. *Anal. Biochem.* **2006**, *350*, 1-23. DOI: 10.1016/j.ab.2005.09.037

[12] Harvey, D. J. *J Chromatogr B* **2011,** *879,* 1196-1226. DOI: 10.1016/j.jchromb.2010.11.010

[13] Vanderschaeghe, D.; Festjens, N.; Delanghe, J.; Callewaert, N. *Biol. Chem.* **2010**, *391,* 149-161. DOI: 10.1515/BC.2010.031

[14] Yodoshi, M.; Tani, A.; Ohta, Y.; Suzuki, S. *J. Chromatogr. A* **2008,** *1203,* 137-146. DOI: 10.1016/j.chroma.2008.07.053

[15] Honda, S.; Suzuki, S.; Kakehi, K. *J. Chromatogr.* **1981,** *226*, 341-350. DOI: 10.1016/S0378-4347(00)86068-5

[16] Honda, S.; Suzuki, S. *Anal. Biochem.* **1984**, *142*, 167-174. DOI: 10.1016/0003-2697(84)90533-5

[17] Wang, W. T.; Ledonne, N. C.; Ackerman, B.; Sweeley, C. C. *Anal. Biochem.* **1984,** *141*, 366-381. DOI: 10.1016/0003-2697(84)90057-5

[18] X. Liu, F. Dahdouh, M. Salgado, F.A. Gomez, *J. Pharm. Sci.* **2009**, *98*, 394-410. DOI: 10.1002/jps.21452.

[19] Heegaard, N. H. H. *Electrophoresis* **2003**, *24*, 3879-3891. DOI: 10.1002/elps.200305668

[20] Bertucci, C.; Bartolini, M.; Gotti, R.; Andrisano, V.; *J. Chromatogr. B* **2003**, *797*, 111-124. DOI: 10.1016/j.jchromb.2003.08.033

[21] Tanaka, Y.; Terabe, S. *J. Chromatogr. B,* **2002**, *768*, 81-92. DOI: 10.1016/S0378-4347(01)00488-1

[22] Duijn, R. M. G.; Frank, J.; van Dedem, G. W. K.; Baltussen, E. *Electrophoresis* **2000**, *21*, 3905. DOI: 10.1002/1522-2683(200012)

[23] Amini, A.; Westerlund, D. *Anal. Chem.* **1998**, *70*, 1425-1430. DOI: 10.1021/ac970766q

[24] de Waard, P.; Koorevaar, A.; Kamerling, J. P.; Vliegenthart, J. F. G. *J. Biol. Chem.* **1991**, *266*, 4237-4243.

[25] Yamamoto, K.; Tsuji, T.; Irimura, T.; Osawa, T. *Biochem. J.* **1981**, *195*, 701-713.

[26] Tsuji, T.; Yamamoto, K.; Irimura, T.; Osawa, T. *Biochem. J.* **1981**, *195*, 691-700.

[27] Charlwood, J.; Birrell, H. ;Organ, A.; Camilleri, P. *Rapid Commun. Mass Spectrom.* **1999,** *13*, 716-723. DOI: 10.1002/(SICI)1097-0231(19990430)13:8<716::AID-RCM547>3.0.CO;2-C

[28] Knibbs, R. N.; Goldstein, I. J.; Ratcliffe, R. M.; Shibuya, N. *J. Biol. Chem.* **1991,** *266*, 83-88.

[29] Kilpatrick, D. C.; Yeoman, M. M. *Biochem. J.* **1978**, *175*, 1151-1153.

[30] Yokoyama, K.; Terao, T.; Osawa, T. *Biochem. Biophys. Acta* **1978,** *538*, 384-396. DOI: 10.1016/0304-4165(78)90366-5

[31] Cummings, R. D.; Kornfeld, S. *J. Biol. Chem.* **1982,** *257*, 11235-11240.

[32] Hammarström, S.; Hammarström, M. L.; Sundblad, G.; Arnarp, J.; Lönngren, J.; *Proc. Natl. Acad. Sci., USA* **1982** , *79*, 1611-1615.

[33] Tazaki, K.; Shibuya, N. *Plant Cell Physiol.* **1989**, *30,* 899-903.

[34] Kornfeld, K.; Reitman, M. L.; Kornfeld, R. *J. Biol. Chem*. **1981**, *256*, 6633-6640.

[35] Teneberg, S.; Angstrom, J.; Jovall, P.; Karlsson, K. *J. Biol. Chem*. **1994**, *269,* 8554-8563.

[36] Yamamoto, K.; Tsuji, T.; Matsumoto, I.; Osawa, T. *Biochemistry* **1981**, *20*, 5894-5899.

[37] Yasmashita, K.; Kochibe, N.; Ohkura, T.; Ueda, I.; Kobata, A. *J. Biol. Chem*. **1985**, *260,* 4688-4693.

[38] Yamashita, K.; Hitoi, A.; Kobata, A. *J. Biol. Chem.* **1983**, *258*, 14753-14755.

[39] Guttman, A. *Nature* **1996,** *380*, 461-462. DOI: 10.1038/380461a0

[40] Fukushima, E.; Yagi, Y.; Yamamoto, S.; Nakatani, Y.; Kakehi, K.; Hayakawa, T.; Suzukia, S. *J. Chromatogr. A,* **2012,** *1246*, 84-89. DOI: 10.1016/j.chroma.2012.02.052

[41] Yamamoto, Y.; Nakatani S.; Suzuki, S. *Anal. Sci.*, **2013**, *29*, 831-835. DOI: 10.2116/analsci.29.831

[42] Zhu, Z.; Zhang, L.; Marimuthu, A.; Yang, Z. *Electrophoresis* **2002**, *23*, 2880-2887. DOI: 10.1002/1522-2683(200209)23:17<2880::AID-ELPS2880>3.0.CO;2-F

[43] Yagi, Y.; Kakehi, K.; Hayakawa, T.; Ohyama, Y.; Suzuki, S. *Anal. Biochem*. **2012**, *431*, 120-126. DOI: 10.1016/j.ab.2012.09.006

[44] Yagi, Y.; Yamamoto, S.; Kakehi, K.; Hayakawa, T.; Ohyama, T.; Suzuki, S. . *Electrophoresis*, **2011**, *32,* 2979-2985. DOI: 10.1016/j.ab.2012.09.006

[45] Weiner, L. M.; Surana, R.; Wang, S. *Nat. Rev. Immunol.* **2010,** *10,* 317-327. DOI: 10.1038/nri2744.

[46] Chan, A. C.; Carter, P. J. *Nat. Rev. Immunol.* **2010,** *10,* 301-316. DOI: 10.1038/nri2761.

[47] Jefferis, R. *Nat. Rev. Drug. Discov*. **2009**, *8*, 226-234. DOI: 10.1038/nrd2804

[48] Kumpel, B. M.; Rademacher, T. W.; Rook, G. A.; Williams, P. J.; Wilson, I. B. *Hum. Antibodies Hybridomas* **1994**, *5*, 143-151.

[49] Kumpel, B. M.; Wang, Y.; Griffiths, H. L.; Hadley, A. G.; Rook, G. A. *Hum. Antibodies Hybridomas* **1995**, *6*, 82-88.

[50] Umana, P.; Jean-Mairet, J.; Moudry, R.; Amstutz, H.; Bailey, J. E. *Nat. Biotechnol.* **1999**, *17*, 176-180. DOI: 10.1038/6179

[51] Davies, J.; Jiang, L.; Pan, L. Z.; LaBarre, M. J.; Anderson, D.; Reff, M. *Biotechnol. Bioeng*. **2001**, *74*, 288-294. DOI: 10.1002/bit.1119

[52] Shields, R. L.; Lai, J.; Keck, R.; O'Connell, L. Y.; Hong, K.; Meng, Y. G.; Weikert, S. H.; Presta, L. G. *J. Biol. Chem*. **2002**, *277*, 26733-26740. DOI: 10.1074/jbc.M202069200

[53] Shinkawa, T.; Nakamura, K.; Yamane, N.; Shoji-Hosaka, E.; Kanda, Y.; Sakurada, M.; Uchida, K.; Anazawa, H.; Satoh, M.; Yamasaki, M.; Hanai, N.; Shitara, K. *J. Biol. Chem.* **2003**, *278*, 3466-3473. DOI: 10.1074/jbc.M210665200

[54] Ma, S.; Nashabeh, W. *Anal. Chem*. **1999**, *71*, 5185-5192. DOI: 10.1021/ac990376z

[55] Kamoda, S.; Rika, I.; Kakehi, K. *J. Chromatogr. A* **2006**, *1133*, 332-339. DOI: 10.1016/j.chroma.2006.08.028

[56] Zhou, Q.; Shankara, S.; Roy, A.; Qiu, H.; Estes, S.; McVie-Wylie, A.; Culm-Merdek, K.; Park, A.; Pan, C.; Edmunds, T. *Biotechnol. Bioeng.* **2008**, *99*, 652-665. DOI: 10.1002/bit.21598

[57] Kanda, Y.; Yamada, T.; Mori, K.; Okazaki, A.; Inoue, M.; Kitajima-Miyama, K.; Kuni-Kamochi, R.; Nakano, R.; Yano, K.; Kakita, S.; Shitara, K.; Satoh, M. *Glycobiology* **2007**, *17*, 104-118. DOI: 10.1093/glycob/cwl057

[58] Wright, A.; Sato, Y., Okada, T.; Chang, K.; Endo, T.; Morrison, S. *Glycobiology* **2000**, *10*, 1347-1355. DOI: 10.1093/glycob/10.12.1347

[59] Millward, T. A.; Heitzmann, M.; Bill, K.; Längle, U.; Schumacher, P.; Forrer, K. *Biologicals* **2008**, *36*, 41-47. DOI: 10.1016/j.biologicals.2007.05.003

[60] Diaz, S. L.; Padler-Karavani, V.; Ghaderi, D.; Hurtado-Ziola, N.; Yu, H.; Chen, X.; Brinkman-Van der Linden, E. C.; Varki, A.; Varki, N. M. *PLoS One* **2009**, *4*, e4241. DOI: 10.1371/journal.pone.0004241

[61] Kamoda, S.; Ishikawa, R.; Kakehi, K. *J. Chromatogr. A* **2006**, *1133*, 332-339. DOI: 10.1016/j.chroma.2006.

08.028

[62] Chen, R. H.; Kadner, A.; Tracy, J.; Santerre, D.; Adams, D. H. *Transplant. Proc*. **2001**, *33* 732-735.

[63] Yamamoto, S.; Watanabe, Y.; Nishida, N.; Suzuki, S. *J. Sep. Sci.* **2011**, *34*, 2879-2884. DOI: 10.1002/jssc.201100423

[64] Yamamoto, S.; Hirakawa, S.; Suzuki, S. *Anal. Chem.*, **2008,** *80* 8224-8230. DOI: 10.1021/ac801245n

[65] Blas, M.; Delaunay, N.; Rocca, J.-L. *Electrophoresis* **2008**, *29*, 20-32. DOI: 10.1002/elps.200700389

[66] Breadmore, M. C. *Electrophoresis* **2007,** *28*, 254-281. DOI: 10.1002/elps.200600463

[67] Abgrall, P.; Nguyen, N. T. *Anal. Chem.* **2008**, *80*, 2326-2341. DOI: 10.1021/ac702296u

[68] Kim, S. J.; Wang, Y. C.; Lee, J. H.; Jang, H.; Han, J. *Phys. Rev. Lett.* **2007**, *99*, 044501. DOI: 10.1103/PhysRevLett.99.044501

[69] Holmes, D. L.; Stellwagen, N. C. Electrophoresis **1991**, *12*, 612-619. DOI: 10.1002/elps.1150120903

[70] Yamamoto, S.; Suzuki, S.; Suzuki, S. *Analyst*, **2012,** *137*, 2211-2217. DOI: 10.1039/C2AN16015C

[71] Okanda F. M.; El Rassi, Z. Electrophoresis, **2006**, *27*, 1020-1030. DOI: 10.1002/elps.200500766

[72] Nakajima, K.; Kinoshita, M.; Matsushita, N.; Urashima, T.; Suzuki, M.; Suzuki A.; Kakehi, K. *Anal. Biochem,* **2006**, *348*, 105-114. DOI: 10.1016/j.ab.2005.10.010

[73] Shimura K.; Kasai, K. *Anal. Biochem*, **1997,** *251*, 1-16. DOI: 10.1006/abio.1997.2212

[74] Meany, D. L.; Hackler, L.; Zhang H.; Chan, D. W. *J. Proteome Res*., **2011,** *10*, 1425-1431. DOI: 10.1021/pr1010873

[75] Kuno, A.; Ikehara, Y.; Tanaka, Y.; Angata, T.; Unno, S.; Sogabe, M.; Ozaki, H.; Ito, K.; Hirabayashi, J.; Mizokami, M .;Narimatsu, H. *Clin. Chem.*, **2011,** *57*, 48-56. DOI: 10.1373/clinchem.2010.151340

[76] Hu S.; Wong, D. T. *Proteomics Clin. Appl.*, **2009**, *3*, 148-154. DOI: 10.1002/prca.200800153

[77] Endo, T.; J. Chromatogr. A, **1996**, *720*, 251-261. DOI: 10.1016/0021-9673(95)00220-0

[78] Madera, M.; Mechref,Y.; Klouckova I.; Novotny, M. V. *J. Chromatogr. B*, **2007**, *845*, 121-137. DOI: 10.1016/j.jchromb.2006.07.067

[79] Mao, X.; Luo, Y.; Dai, Z;. Wang, K.; Du Y.; Lin, B. *Anal. Chem*, **2004**, *76*, 6941-6947. DOI: 10.1021/ac049270g

[80] Dhuna, V.; Bains, J. S.; Kamboj, S. S.; Singh, J. S.; Kamboj A.; Saxena, K. *J. Biochem. Mol. Biol,* **2005,** *38*, 526-532.

[81] Gupta A.; Sandhu, R. S. *Mol. Cell. Biochem,* **1997**, *166,* 1-9.

[82] Clegg, R. M.; Loontiens, F.G.; Van Landschoot A.; Jovin, T. M. *Biochemistry,* **1981,** *20,* 4687-4692.

[83] Mega, T.; Oku H.; Hase, S. *J. Biochem.* (Tokyo), **1992**, *111*, 396-400.

[84] Honda, S.; Suzuki, S.; Nitta T.; Kakehi, K. *J. Chromatogr.,* **1988,** *438*, 73-84. DOI: 10.1016/S0021-9673(00)90234-6

[85] Suzuki, S.; Fujimori, T.; Yodoshi, M. *Anal. Biochem.* **2006**, *354*, 94-103. DOI: 10.1016/j.ab.2006.04.013

[86] France, R. R.; Cumpstey, I.; Butters, T. D.; Fairbanks, A. J.; Wormald, M. R. *Tetrahedron Asymmetry* **2000**, *11*, 4985-4994. DOI: 10.1016/S0957-4166(00)00477-8

[87] Anumula, K. R.; Du, P. *Anal. Biochem*.**1999,** *275*, 236-242. DOI: 10.1006/abio.1999.4323

[88] Kinoshita A.; Sugahara, K. *Anal. Biochem*. **1999**, *269*, 367-378. DOI: 10.1006/abio.1999.4027

[89] Hase, S.; Ikenaka, T.; Matsushima, Y. *J. Biochem.* **1979,** *85*, 989-94.

[90] Jackson P. *Anal. Biochem.* **1994**, *216*, 243-252. DOI: 10.1006/abio.1994.1038

[91] Kallin, E. *Methods Enzymol*. **1994**, *242*, 119-123.

[92] Kallin, E.; Lönn, H.; Norberg,T. *Glycoconjugate. J.* **1988,** *5*, 145-150.